

# We are IntechOpen, the world's leading publisher of Open Access books Built by scientists, for scientists

6,900

Open access books available

185,000

International authors and editors

200M

Downloads

Our authors are among the

154

Countries delivered to

TOP 1%

most cited scientists

12.2%

Contributors from top 500 universities



WEB OF SCIENCE™

Selection of our books indexed in the Book Citation Index  
in Web of Science™ Core Collection (BKCI)

Interested in publishing with us?  
Contact [book.department@intechopen.com](mailto:book.department@intechopen.com)

Numbers displayed above are based on latest data collected.  
For more information visit [www.intechopen.com](http://www.intechopen.com)



---

# Carbon Nanotube (CNT)-Reinforced Metal Matrix Bulk Composites: Manufacturing and Evaluation

---

Sebastian Suárez, Leander Reinert and  
Frank Mücklich

Additional information is available at the end of the chapter

<http://dx.doi.org/10.5772/63886>

---

## Abstract

This chapter deals with the blending and processing methods of CNT-reinforced metal matrix bulk composites (Al/CNT, Cu/CNT and Ni/CNT) in terms of solid-state processing, referring mainly to the research works of the last ten years in this research field. The main methods are depicted in a brief way, and the pros and cons of each method are discussed. Furthermore, a tabular summary of the research work of the mentioned three systems is given, including the blending methods, sintering methods, the used amount of CNTs and the finally achieved relative density of the composite. Finally, a brief discussion of each system is attached, which deals with the distribution and interaction of the CNTs with the matrix material.

**Keywords:** Carbon nanotubes, metal matrix composites, reinforcement effect, solid-state processing.

---

## 1. Introduction

Composite materials have been in the spotlight of material science and engineering for a long time already. They provide the capability of tailoring their properties by managing very simple variables such as the reinforcement fraction or the processing parameters, among others. Their application area is found in a wide range of dissimilar fields, ranging from bioengineering [1,2] up to aerospace [3]. The applicability relies on the proper selection of both, the matrix phase and the reinforcing phase. By matrix, the phase with the largest volume fraction is meant, whereas the opposite is valid for the reinforcing phase. In the former – according to the specific application – polymers, ceramics or metals are used. Polymer-matrix composites are mainly used in

applications where lightweight is required, working in environments that do not present high temperatures. On the opposite, ceramic matrices are used where inertness under high temperatures is required as well as high mechanical properties. Finally, metal matrix composites (MMC) lie in between both application fields, presenting in most cases tailored microstructures (and subsequently, tailored physical properties) and, in certain cases, lightweight.

Reinforcing phases can be of very dissimilar nature. The most widespread phases are usually ceramic fibres and/or particles (i.e.  $\text{Al}_2\text{O}_3$ , TiC), which show very good mechanical properties, thus enhancing the overall mechanical properties of the composite. However, when considering the transfer properties (electrical and thermal), their ceramic nature plays a detrimental role. Furthermore, the fact that the material being subjected to improvement is a metal, with usually very good transport properties, the task becomes indeed non-trivial.

In recent years, the appearance of carbon nanotubes (CNTs) has opened an interesting new field. Since CNTs show intrinsically outstanding physical properties, the aforementioned drawback brought by ceramic reinforcements might be straightforwardly overcome. Yet, the predicted physical properties of CNTs are only realisable if the CNT is in a “perfect” structural state. By “perfect” structural state, it is meant that there are (a) no structural defects on its lattice, (b) no exo- or endohedral contaminants (synthesis/catalysis residues) and (c) the CNTs are in an isolated state (no CNT agglomeration). Those three conditions are quite challenging to achieve in the praxis.

When it comes to CNTs, different synthesis methods have to be considered. CNT synthesis renders unavoidably contaminants (sulphur/amorphous carbon) and catalyst particles. The most common synthesis methods employed are chemical vapour deposition (CVD), arc discharge and laser ablation. The CVD synthesis is the one with the highest capacity to be scaled to industrial quantities and provides a better control on the morphology of the obtained CNTs [4,5] in comparison with other standard synthesis methods. Yet, the defect state is usually high and should be thoroughly analysed before the application.

Most of the recent research works are leaning towards commercially available MWCNTs as starting material for the composite production. Some of the most recurring suppliers are Nanocyl (Belgium), Nanolab Inc. (USA), Iljin Nanotechnology Co. Ltd (Korea), Bayer MaterialScience (Germany), Chengdu Organic Chemicals Co. Ltd (China), Chinananotech Co. Ltd (China) and Hanhwa Nanotech Co. Ltd (Korea) to name just a few [6–31]. But also self-produced CNTs are used for composite manufacturing. For this purpose, catalytic chemical vapour deposition (CCVD) is the most common way to synthesize CNTs that are used as reinforcement phase in composites [6,7,10,32–39]. The MWCNTs generally show a purity between 90% [10] and 99.5% [19], but mostly around 95%. The diameter ranges from 10 nm to 80 nm with a length of 0.5  $\mu\text{m}$ –50  $\mu\text{m}$  [6–39]. All the information about CNT-MMCs in this book chapter is derived from the research works of the last ten years, including some relevant exceptions.

## 1.1. Blending methods

Considering that commercial CNTs are usually delivered in agglomerated form, different methods have to be employed to disaggregate and blend them with the metallic matrix material. There are a lot of dispersing and blending processes like magnetic stirring [40], nanoscale dispersion processing [18,21,41], colloidal mixing [6,16,22,26–31,41–49], molecular-level mixing [7,9,11,12,14,24,25,50–54], particle composite system mixing [15,55], friction stir processing [56], layer stacking [57], ball milling [8,10,17,19,20,22–24,32–36,38,50,53,58–74], dipping [75] or roller mixing [37,76]. However, three of them have to be pointed out as the most commonly used ways to disperse and blend CNT metal matrix systems. These three processing methods are ball milling, molecular-level mixing and colloidal mixing. The methods will be briefly commented in the following paragraphs.

### *Ball milling*

It is usually performed using a planetary or attrition ball mill. The mixing is done by filling in the Metal powders and reinforcement phase together with some hard balls into mixing jars and rotating the jar with a certain rotational speed (**Figure 1 a**).

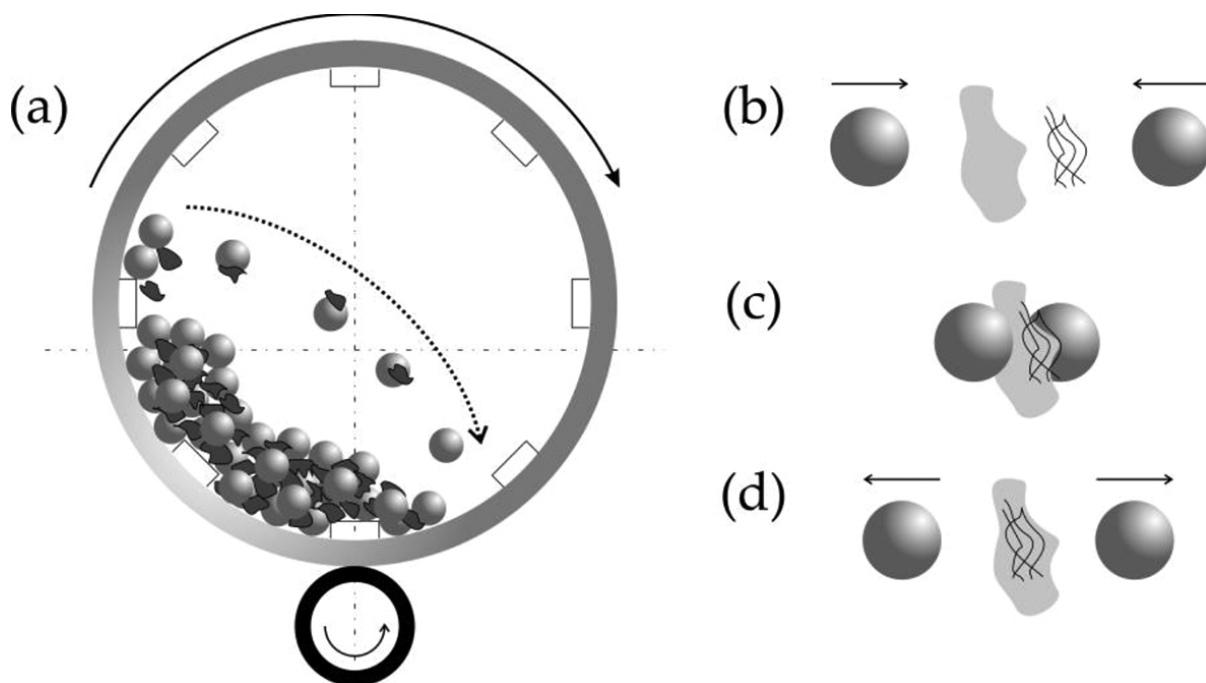


**Figure 1.** Schematic draft of the ball milling process (a). The used balls are hitting the CNTs and the matrix powder material (b), welding and integrating the two components (c) and bounce of the powder particle to restart this process again at another spot (d).

During the rotational movement, the added balls are falling on top of the powder material (**Figure 1 b**), thus leading to a size reduction, particle welding and integration of CNTs into the matrix powder material (**Figure 1 c and d**) generated by the impact energy. Different ball materials and sizes, rotational speeds, balls to powder ratios, gas atmospheres and mixing

times can be chosen as main mixing parameters. Usually, a process control agent, for example ethanol, is added in order to prevent cold welding of the matrix material powder particles. In other cases, like mechanical alloying, a cold welding of the particles is desired. Ball milling is known to produce a homogenous distribution of reinforcement phase in metal matrix composites as particle agglomerates are segmented, and dispersed CNTs are partially welded together with the matrix powder material (**Figure 1 d**). In general, high energy ball milling and low energy ball milling are distinguished in literature when it comes to the mixing process of CNTs with metal matrix material. This is because of the main drawback of the method, which is the increasing defect density of CNTs during the mixing process by the direct application of large contact pressures (up to 30 GPa) [77]. Using low energy ball milling, this unwanted effect can be reduced, but it will not vanish. The importance of a low defect density of CNTs will be discussed later on in entry 2.2 [8,10,17,19,20,22–24,32–36,38,50,53,58–74].

### *Molecular-level mixing*

For this mixing method, it is of utmost importance to functionalize the CNTs, for example with an acid treatment (**Figure 2 a**). After this, the CNTs can be dispersed in various solvents, for example using ultrasonic agitation to obtain a stable suspension.

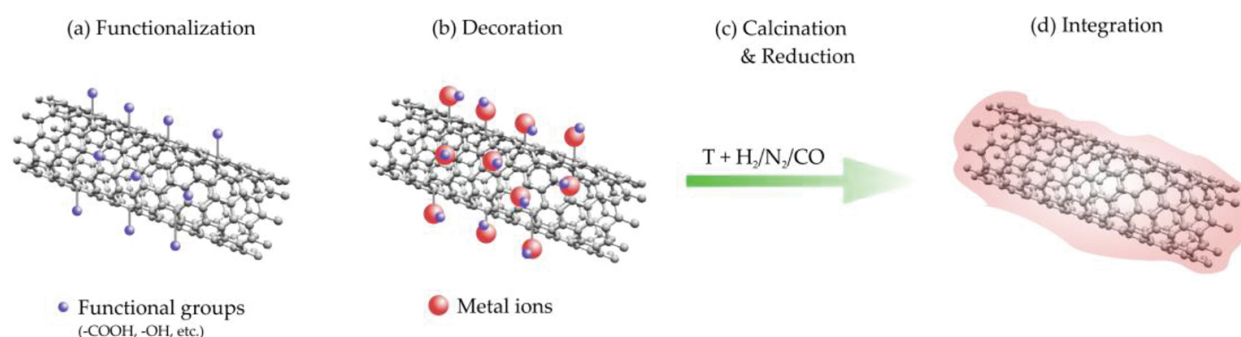


**Figure 2.** Schematic draft of the molecular-level mixing method. CNTs are functionalized by functional groups, which will be covalently bond onto the CNTs surface (a). After this, metal ions can electrostatically interact with the functional groups, thus coating the CNT surface with metal ions (b). These ions are transformed to a pure metal layer by calcination and reduction under temperature and  $H_2$ ,  $N_2$  or CO atmosphere (c). Finally, the CNTs are fully decorated or even integrated in the metal matrix material (d).

A metal salt is added and reduced by an added reducing agent to form a metal oxide CNT suspension with the CNTs acting as nucleation centres for the metal oxide formation (**Figure 2 b**). Finally, after washing off all the remaining chemicals, the powder is calcinated and then reduced, for example under hydrogen atmosphere to reduce it to the metal/CNT powder (**Figure 2 c and d**). The advantage of this process is that the CNT particles are embedded or coated by the metal matrix, thus resulting in very homogeneous distributions within the metal matrix (**Figure 2 d**). In many other mixing methods, the reinforcement phase can only be situated at the grain boundaries, offering weak interfacial bonding between the reinforcement phase and the matrix material and reducing the homogeneity of the distribution. For the molecular-level mixing process, this is not true, therefore being favoured for applications where a good connectivity of the reinforcement phase network is needed like thermal or



electrical applications. The main drawback of the method is the required functionalization, which involves breaking up covalent carbon bonds to add functional groups to the surface of CNTs, thus diminishing their outstanding properties [7,9,11,12,14,24,25,50–54].

### *Colloidal mixing*

For colloidal mixing, the CNTs are dispersed using an ultrasonic bath, homogenizer or magnetic stirrer in a solvent (for the most part, ultrasonic agitation is used (**Figure 3 a**)). There are many different solvents that allow for a fine and stable dispersion of the CNTs, which is discussed in [81] (e.g. DMF or ethylene glycol). The dispersion grade and stability of the CNT suspensions are not only depending on the used solvent, but also on the surface of the used CNTs. Some research works functionalize the surface of the CNTs to obtain electrochemically stable dispersions, which works great but influences the physical properties of CNTs as already discussed for the molecular-level mixing. Other works avoid functionalization, thus using the pristine CNTs, retaining their properties in detriment of the dispersion quality.

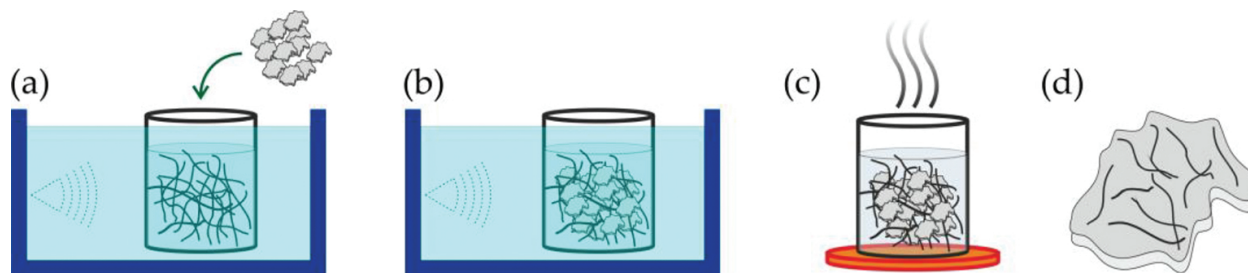


**Figure 3.** Schematic draft of the colloidal mixing method. First, the CNTs are dispersed in a liquid solvent using ultrasonic agitation, after which the matrix material powder is added (a). The two components are mixed again by ultrasonic agitation (b), and the solvent is evaporated (c) to finally obtain the mixed CNT/metal matrix powder (d).

One point that is controversially discussed is the impact of ultrasonic agitation on the defect density of CNTs. There are studies claiming for a rise in the defect density as a function of the time spent in the ultrasonic bath and others which report the opposite. The observed decrease in the defect density might be a misinterpretation of Raman spectra of disentangled CNTs (which would render improved  $I_D/I_G$  ratio stemming from the avoidance of intertube interactions). After the dispersion of CNTs in the solvent, the metal powder is added and mixed with the dispersed CNTs again by ultrasonic agitation, stirring or a homogenizer (**Figure 3 b**). Finally, the solvent is evaporated to obtain a dry mixed powder (**Figure 3 c and d**). A significant advantage of this method is that it can be very easily upscaled and still yield the same results [6,16,22,26–31,41–49].

## **1.2. Processing methods**

After merging the CNT/metal composite powders, different densification methods are used for the consolidation of the final samples. Examples of these are cold pressed sintering (CPS) [8,14,17,20,27,28,34,35,47,53,63,74,78], hot uniaxial pressing (HUP) [10,19,26,27,29–31,39,40,47,49,62,67–70], spark plasma sintering (SPS) [6,7,9,11,12,14–16,18,21,23–25,42,44–46,48,50–52,55,

64,75,79,80], hot or cold rolling [7,50,59,60,64], hot extrusion [18,20,23,40,58,79], high pressure torsion (HPT) [22,31–33,41,54,61,65,66,71,73], friction stir processing [56], hot isostatic pressing (HIP) [22,57], microwave sintering [43], laser engineered net shaping (LENS) [36–38,76] or a combination of those methods. Methods like cold or hot rolling, hot extrusion or HPT are often used for post-processing of the already consolidated samples [7,22,31,50,59,60,64]. The most often used methods for the production of metal matrix composites are CPS, HUP and SPS, which will be described briefly in the following.

#### *Cold Pressed Sintering (CPS)*

This is by far the simplest method to densify the blended powder. Using a uniaxial press or an isostatic press, the powder is pre-compacted to the desired shape (**Figure 4**).

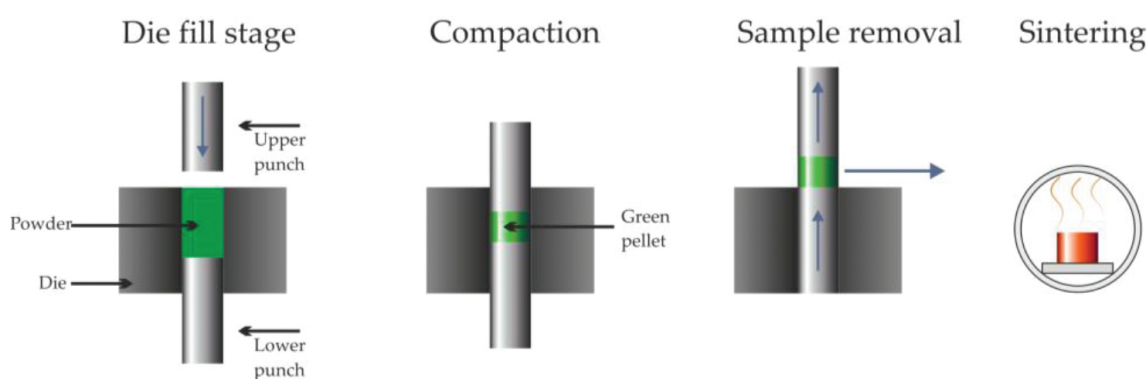


**Figure 4.** Schematic draft of pressureless sintering or cold pressed sintering. A die is filled with the powder material, which is then pressed uniaxial to a green pellet. The sample is then removed and sintered without pressure in a furnace under vacuum or inert gas atmosphere.

After this, the sample is sintered without further pressure under vacuum or an inert gas atmosphere to form the consolidated sample (**Figure 4**). Even though one heating–cooling cycle might be very time-consuming (the resistive furnaces usually have a very limited heating rate), it has the advantage that many samples of dissimilar shapes can be sintered at the same time, making this sintering method very time efficient. However, the densification mechanism is mainly based on lattice and grain boundary diffusion [81], and large porosities cannot be closed without applying pressure, thus resulting in a poor final density of the composite [8,14,17,20,27,28,34,35,47,53,63,74,78].

#### *Hot Uniaxial Pressing (HUP)*

In addition to lattice and grain boundary diffusion (mechanisms for pressureless sintering), plastic deformation and creep can be major sintering mechanisms. As the overall densification rate of a compact is a function of the sum of the active densification mechanisms, pressure-assisted sintering is much more effective than pressureless sintering. The application of an external pressure leads to an increase in the densification driving force and kinetics. As grain growth is not related to the applied external pressure, it is more effective in systems with a

large grain growth to densification rate. To sum up, by using an external pressure, the sintering temperature as well as the sintering time can be reduced [81].

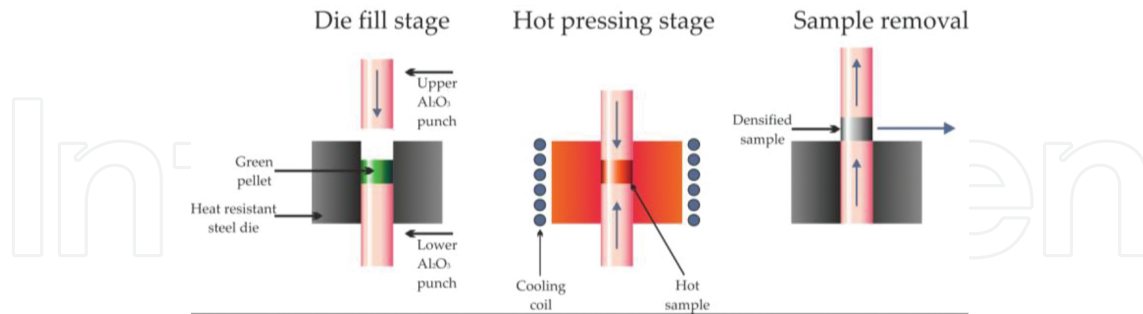


**Figure 5.** Schematic draft of the hot uniaxial pressing method. A pre-compacted green pellet is inserted in a die, and uniaxial pressure is applied while the pellet is heated by induction under vacuum or inert gas atmosphere. The densified sample is finally removed.

When it comes to HUP, as with the CPS method, the mixed powder is usually pre-compacted using a uniaxial press or an isostatic press to obtain green pellets. After this, the green pellets are typically inserted in a die (often a steel die) where two punches (e.g. alumina) exert a uniaxial pressure onto the sample (**Figure 5**). The heating of the sample is usually conducted by induction, and thus, this system is very limited in the heating rate, rendering HUP as a very time-consuming sintering process. However, high pressures (several hundred MPa) can be applied with this method while sintering and almost full densification can be achieved (as punches with good mechanical properties can be used). To conclude, HUP is a time-consuming way to sinter samples, but it is also very effective when it comes to the final maximum densification of the sample [10,19,26,27,29–31,39,40,47,49,62,67–70].

### *Spark Plasma Sintering (SPS)*

The active sintering mechanisms in SPS do not vary much from the active mechanisms in HUP. Yet, it provides a much quicker way to consolidate the composite powders [81].

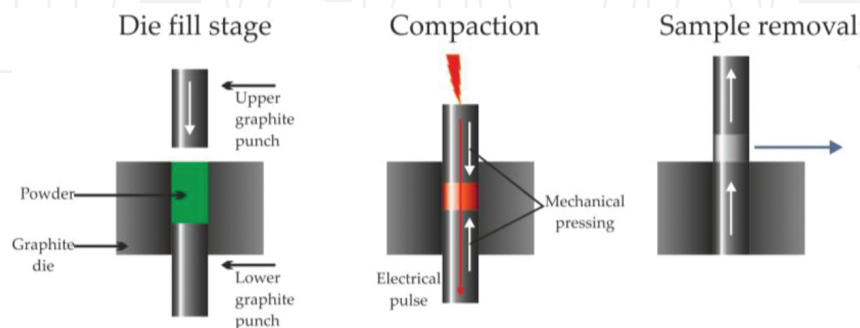


**Figure 6.** Schematic draft of the Spark plasma sintering method. A graphitic die is filled with the powder material, and a uniaxial pressure is applied via two graphite punches. A pulsed electric DC is applied, which leads to the heating of the sample by its electrical resistance. The process is conducted under vacuum or inert gas atmosphere.



As with HUP, the mixed powders are pre-compacted using a uniaxial press or an isostatic press to obtain green pellets, which are inserted in a graphite die. With this method, graphite punches are used to allow for inducing a pressure at the sample and conducting a pulsed electric DC through the sample at the same time (**Figure 6**). The sample is heated by its electrical resistance, which depends on the used material. By controlling the used current, the heating rate can be adjusted. This method allows for a very high heating rate of several hundred °C/min, being therefore very time efficient. In contrast to HUP, the used pressure during sintering is much lower (typically about 50 MPa) because of the mechanically weak graphite punches. However, as with HUP, almost full densification can be reached with this method. Overall, this method offers a quick and effective way to consolidate the CNT-reinforced metal matrix powders, therefore being the most employed method in this area [6,7,9,11,12,14–16,18,21,23–25,42,44–46,48,50–52,55,64,75,79,80].

### 1.3. Potential applications

The main application of the CNT-reinforced metal matrix composites is in structural applications. This is due to the fact that most of the literature is devoted to the study of the mechanical properties of the composites. From the mechanical point of view, the addition of an intrinsically strong second phase would certainly improve the overall properties. Considering that, in the ideal state, the CNTs show a Young's modulus of approximately 1 TPa and a maximum tensile strength of over 60 GPa [82], it is easy to trace their influence. Additionally, a set of factors influences the mechanical behaviour of these composites. First, it has been demonstrated that the addition of CNTs acts on the grain boundary mobility by hindering their displacement during grain growth [83–85]. This effect influences the final microstructure (by refining it) and thus the mechanical behaviour (grain boundary strengthening). Second, a proper distribution of CNTs acts as an obstacle for dislocation movement, activating another strengthening mechanism known as particle dispersion strengthening (Orowan strengthening). Third, it has been shown that the CNTs present a very low or even negative coefficient of thermal expansion (CTE) in a wide temperature range [86,87]. When combined with high CTE materials (such as metals), this CTE mismatch acts also as a strengthening factor. Finally, considering the aforementioned values of the mechanical properties of the CNTs, the strengthening of the composite due to load transfer is expected to be significant. Summarizing, the addition of CNTs to MMCs is clearly expected to be beneficial in terms of the improvement of the mechanical behaviour, and subsequently, it is clear why most of the studies are focused towards this feature. The strengthening effect of the CNTs in MMCs is shown in **Figure 4**. There, the measured yield strength improvement of different systems is given as a function of the CNT volume concentration in the composite. The scattering of results is related to the different mixing and processing methods that were employed. In this context, it becomes clear that after a direct comparison of different research works involving a wide span of production methods for the same system, the task of correlating dissimilar results becomes non-trivial. Due to a lack of available information on the yield strength of Ni-CNT composites, this illustration provides only a summary of the mechanical reinforcement effect that was achieved so far with Al-CNT and Cu-CNT MMC systems.

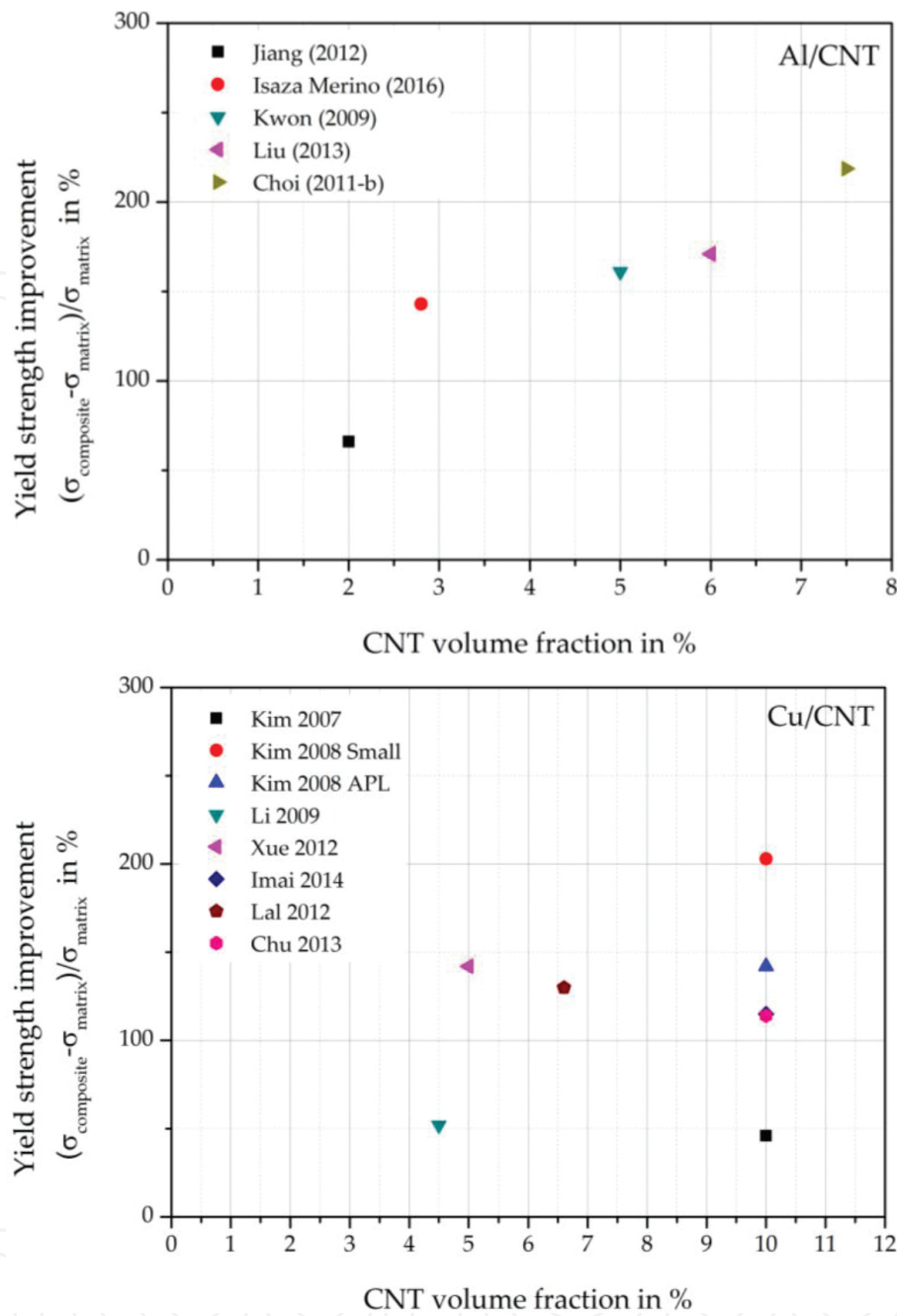


**Figure 7.** Yield strength improvement against the volume fraction of CNTs in (a) Al/CNT composites [18,20,56,57,60] and (b) Cu/CNT composites [7,9,11,53,64,66,70,75].

However, the transport properties occupy also a large amount of the research in this field. CNTs are predicted to have the highest thermal conductivity known (SWCNT: 6600 W/m.K [88], MWCNT: 3000 W/m.K [89]) and are expected to present a ballistic type of electrical conduction mechanism [90,91]. Both factors are of utmost importance when considering that the material to be improved is a metal (which usually shows very high thermal and electrical properties). However, it is critical to obtain individual CNTs after dispersion, since the transport properties could be reduced up to one order of magnitude If the CNTs are in

agglomerated form [92]. In this regard, some parts of the research on Cu-CNT were aimed at the improvement of the thermal properties. Cho et al. observed an improvement of the thermal conductivity for very low CNT concentrations (up to 1 vol. %) [42]. For larger CNT concentrations, the agglomeration of CNTs starts to play a fundamental role in the conductivity decrease. The same effect was observed by Yamanaka et al. for Ni-CNT [46]. Inversely, Firkowska et al. tested several functionalization routes so as to improve the interface in Cu-CNT composites and thus the thermal transport [14]. They observed that for all cases, the degradation of the CNT's intrinsic thermal properties was so relevant and that it was not able to increase the thermal conductivity of the composites in any case.

The electrical behaviour was also studied in several MMC-CNT systems, usually resulting in reduced conductivity. The major factor influencing this behaviour is the presence of agglomerates that, analysed from an electrical transport point of view, are seen as voids. This happens mainly due to the fact that the interfaces between CNT agglomerates and the metal matrices are weak. Only marginal improvements in conductivity were observed for low CNT concentrations in Ni/CNT composites [46].

The tribological properties of CNT-reinforced composites have also been reported in the literature. In most cases, a reduction in both the coefficient of friction (COF) and wear has been observed. In the case of Ni-CNT composites, the COF was reduced in margins from 40 [37] to 75 % [27]. Regarding the Cu-CNT system, the COF reductions ranged from 50 to 75 % [6,8,43, 51,63]. For both systems, the reduction in wear losses achieved in certain cases up to 6 [51], 7 [27] and 8 [43] times that of the reference metal under the same experimental conditions.

The former is usually traced back to a solid lubricant activity of the CNTs during the experiments [37]. Due to their high mechanical properties, they tend to act as rolling second phases at the interface between the rubbing surfaces, thus avoiding the direct contact between the surfaces. In some cases, also the development of a graphitic layer is observed, acting as a solid lubricant [37]. The wear reduction is mainly correlated to the increase in the mechanical properties of the composite, which—as already stated—is generated by a stabilization of the microstructure due to grain boundary pinning. Moreover, Kim et al. stated that a reduction in the wear loss might be due to the reduction in the grain peeling mechanism due to a CNT anchoring of the matrix grains [51].

## **2. Aluminium/CNT system**

### **2.1. Solid-state processing**

Al/CNT composites are mainly interesting, because of their high potential being a lightweight, reinforced material, which can be used in manifold applications. Therefore, Al/CNT composites have been in the focus of research since 1998 [40] and the interest is still growing.

There is a large variety of starting materials on the market that have been used to fabricate the composites. Some of the most mentionable suppliers for Al powders are ECKA Granules Japan Co. Ltd (Japan), Aluminium Powder Company Ltd (United Kingdom), Alpha Industries

(South Korea) and AlfaAesar (Germany) [18,19,21,58,61,62]. The range of used powders goes from several  $\mu\text{m}$  up to  $75\ \mu\text{m}$  in mean particle size, having different particle shapes and various purity grades between  $>99\%$  and  $>99.99\%$  [18,22,39–41,50,56–59,79]. The most used blending method for Al/CNT composites is ball milling [19,20,22,23,50,58–62].

A detailed overview of the research papers in the Al/CNT composite manufacturing can be found in **Table 1**.

Reference	Blending method	Sintering method	CNT content Value wt%	Relative density Value %
Kuzumaki et al. (1998) [40]	<b>Stirring:</b> Stirring in ethanol at 300 rpm for 0.5h, drying in vacuum furnace.	<b>HUP and hot extrusion:</b> Packed in an Al case and preheated for 1.5 h at 873 K in vacuum (0.53 Pa) and then compressed with 100 MPa in steel dies for 60 min. The heating and loading rates were 29.1 K/min and 10 MPa/min, respectively. Then, the composites are extruded at 773 K (extrusion ratio = 25 : 1) at a speed of 10 mm/min	5 vol% 10 vol%	94% 96.2%
Xu et al. (1999) [39]	<b>Hand grinding:</b> For $> 30$ min.	<b>HUP:</b> At 793 K under a pressure of 25 MPa for more than 30 min.	1 wt% 4 wt% 10 wt%	XXX
Tokunaga et al. (2008) [41]	<b>Colloidal mixing process:</b> Mixing by sonication for 5min and then evaporation of the solvent.	<b>HPT:</b> At room temperature with an applied pressure of 2.5GPa. The rotation is initiated 5s after the load application and terminated after 30 turns.	5 wt%	98.4%
Kwon et al. (2009) [18]	<b>NSD:</b> Consisting of commercial gas atomized Al powder, CNTs and natural rubber. The precursor is heat treated at $500\ ^\circ\text{C}$ for 2 h in an argon atmosphere (1 l/min) to evaporate the natural rubber.	<b>SPS and hot extrusion:</b> Sintering at $600\ ^\circ\text{C}$ , holding time of 20 min, heating rate of $40\ ^\circ\text{C}/\text{min}$ and pressure of 50 MPa. The sintered compact was extruded in a $60^\circ$ conical die at $400\ ^\circ\text{C}$ with a pressure of 500 kN. The extrusion velocity and the extrusion ratio were fixed at 2mm/min and 20, respectively.	5 vol%	Sintered: 96.1% Hot extruded: 98%
Esawi et al. (2009) [58]	<b>Ball milling:</b> At 200 rpm for 3h and 6h using 75 stainless steel milling balls (10mm diameter); giving a ball-to-powder weight	<b>Hot extrusion:</b> Compacted at 475MPa. Hot extrusion of the compact is conducted at $500^\circ\text{C}$ using an extrusion ratio of 4:1.	2 wt%	XXX

Reference	Blending method	Sintering method	CNT content Value wt%	Relative density Value %
	ratio of 10:1. The jars are filled with argon and 2ml of methanol is added.			
<b>Kwon et al. (2010)</b> [79]	<b>NSD:</b> Consisting of commercial gas atomized Al powder, MWCNTs and natural rubber. The precursor was heat treated at 500 °C for 2 h in an argon atmosphere (1 l/min) to evaporate the natural rubber.	<b>SPS and hot extrusion:</b> Sintered at 480, 500, 560, and 600°C with a heating rate and holding time of 40 °C/min and 20 min, respectively. A pressure of 50 MPa is used. SPSed compacts were extruded in a 60° conical die at 400 °C with a 500 kN press. The extrusion velocity and extrusion ratio were fixed at 2mm/min and 20, respectively.	1 vol%	Up to 96.8%
<b>Choi et al. (2011)</b> [59]	<b>Ball milling:</b> A2024 chips are ball-milled at 500 rpm under argon atmosphere for up to 48 h. The ball-to-chip weight ratio was 15:1. A control agent of 1.0 wt% stearic acid is added. The composite powder is then produced by ball-milling 18-h A2024 powder and CNTs	<b>Hot rolling:</b> Heated to a temperature of 450 °C and then hot rolled with every 12% reduction per a pass; the initial thickness was 20mm, and the final thickness was 1 mm.	1 vol% 2 vol% 3 vol%	XXX
<b>Choi et al. (2011)</b> [60]	<b>Ball milling:</b> Aluminium powder was solely ball-milled for 18h or 12h and then mixed with CNTs by ball-milling for 6h. Or Aluminium powder is directly mixed with CNTs by ball milling for 6h.	<b>Hot rolling:</b> Heated to a temperature of 450°C, 480°C or 530°C and then hot rolled with every 12% reduction per a pass; the initial thickness was 20mm and the final thickness was 1 mm.	1.5 vol% 3 vol% 4.5 vol% 6 vol% 7.5 vol% 9 vol%	96.3%- 99.9% depending on parame ters.
<b>Kwon et al. (2011)</b> [19]	<b>Ball milling:</b> For 3h under an argon atmosphere; 360 rpm, Ø 10mm ball, 10:1 ball to powder weight ratio, and 20 wt% heptane was used as the process control agent.	<b>HUP:</b> Consolidating at 500 °C for 5min under a uniaxial pressure of 57 MPa.	5 vol% 10 vol% 15 vol%	100%
<b>Jiang et al. (2012)</b> [20]	<b>Ball milling:</b> Flake powder is obtained by ball milling of near-spherical powder with an initial ball-to-powder weight ratio	<b>CPS and Hot extrusion:</b> Compacted under 500 MPa pressure, and then sintered in flowing Ar atmosphere at 550 °C for 2h.	0.5 vol% 2 vol%	After CPS: 80-85% After



Reference	Blending method	Sintering method	CNT content Value wt%	Relative density Value %
	of 20:1 and 423 rpm for several hours in flowing Ar atmosphere with water cooling. The as-prepared Al nanoflakes are first surface modified by PVA with 1700–1800 repeat units and then mixed with a CNT suspension, which is then heated in flowing Ar atmosphere at 500 °C for 2 h to remove the PVA. 1kg blend in 8 hours.	Then heated to 440 °C with a heating rate of 10 °C/min within a vacuum furnace installed with the extruder. And extruded with an extrusion ratio of 20:1 at a ram speed of 0.5 mm/min.		hot extrusion: > 99.5%
Nam et al. (2012) [50]	<b>Molecular-level mixing and ball milling:</b> Poly-vinyl alcohol aqueous solution and CNTs are mixed by tumbler ball milling for 48 h, followed by drying in vacuum at 100 °C. The PVA-coated CNTs, $\text{Cu}(\text{CH}_3\text{COO}) \cdot 2 \text{H}_2\text{O}$ and 2 M NaOH aqueous solution are dispersed in water and heated to 80 °C to form a CNT/CuO composite. This is followed by vacuum filtering and reduction at 300 °C under a hydrogen atmosphere. CNT/Cu composite powders and Al powders are then mixed using a planetary mill for 3 h with rotation speed of 200 rpm; the ball to powder ratio was 10:1. The composition of the Al–Cu matrix is Al-4wt%.	<b>SPS and cold rolling:</b> Sintered at 500 °C for 5 min in a vacuum of $10^{-3}$ torr under a pressure of 50 MPa . The CNT/Al–Cu composites are solution heat treated at 550 °C for 12 h and quenched in a water bath at room temperature. They were then cold rolled to achieve 5% plastic deformation. The composites are finally aged at 130 °C for 0 to 24 h.	2 vol% 4 vol%	XXX
Kwon et al. (2013) [21]	<b>NSD:</b> The precursor was heat-treated at 500°C for 2 h in an argon atmosphere (1 l/min) in order to evaporate the natural rubber.	<b>SPS:</b> Sintering at 600 °C, holding time 20 min, heating rate 40 °C/min, and pressure 50 MPa. Then heat-treated in an alumina pan at 670 °C and at 800 °C for 1 h in an argon atmosphere (1 l/min) inside a tube furnace.	5 vol%	96%
Liu	<b>Friction stir processing (FSP):</b>	<b>Friction stir processing:</b> A	1.6 vol%	XXX

Reference	Blending method	Sintering method	CNT content Value wt%	Relative density Value %
et al. (2013) [56]	Plates of aluminium alloy are used as the substrate materials. Holes with a depth of 3.5 mm and a diameter of 0 mm, 2 mm, 4 mm, 6 mm, 8 mm and 10 mm respectively were drilled in the aluminium plates, which are then filled with various quantities of CNTs.	tilt angle of 2° is applied on the fixed pin tool during FSP. The pitch distance was 0.3 mm. The forward velocity of the rotating pin is kept as a constant of about 30 mm/min, and a rotational speed of 950 rpm is used. Five passes on the same position were conducted on each plate.	2.5 vol% 4.4 vol% 5.3 vol% 6 vol%	
Asgharzadeh et al. (2014) [61]	<b>Ball milling</b>	<b>HPT:</b> Pre-compacted under pressure of ~1 GPa. Then, the green compacts are compressed and deformed under the applied pressure of 6 GPa at room temperature. The rotation of the lower anvil was started after 30 seconds of load application with a rotational speed of 1 rpm and was terminated after various numbers of revolutions up to 15.	3 vol%	98.5% - 99.5%
Phuong et al. (2014) [22]	<b>Colloidal mixing and Ball milling:</b> CNTs are functionalized and dispersed in ethanol by sonication. Then, Al powders and CNT suspension were mixed by mechanical stirring and simultaneously heated in order to evaporate most of the ethanol. The slurry is then processed in a high energy ball mill for 2 h with 250 rpm. Drying is accomplished at 60 °C using a vacuum oven.	<b>HIP and HPT:</b> After cold compaction, capsule free method HIP is accomplished under pressure of 103 MPa, at 600 °C for 30 min. Straining was carried out at room temperature, by torsion to 5 revolutions, under pressure of about 5 GPa and at rotation speed of 2 rpm. The specimens are then annealed in vacuum for 3 h at temperatures of 100 °C, 150 °C, 200 °C and 250 °C.	0.5 vol% 1 vol% 1.5 vol% 2 vol%	XXX
Isaza Merino	<b>Layer stacking:</b> CNTs are added to a solution	<b>HIP:</b> In argon atmosphere . The pressure and temperature are	0.5 wt% 2 wt%	XXX

Reference	Blending method	Sintering method	CNT content Value wt%	Relative density Value %
et al. (2016) [57]	composed of 4 wt.%, PVA dissolved in distilled water. This mixture is magnetically stirred at 1000 rpm during 1 h, followed by a sonication at energies between 40 and 60 kJ and a power of 100W. Finally, this mixture is cured at room temperature in a Petri dish for 8 days. The composite sheets are cut into small sections and stretched at a rate of 2mm/min in a tensile machine at 80 °C. Then, two composite sheets of polymer/CNTs are alternately stacked with three aluminium sheets.	raised gradually during 1.5 h to 40MPa and 650 °C for 30 min. This allows for the evaporation of PVA and aluminium diffusion between the sheets to finally produce the consolidation of the composite.		
Carvalho et al. (2016) [62]	<b>Ball milling:</b> Al-Si 88-12 wt% and CNTs are mixed using 12 steel milling balls with 10-mm diameter, presenting a ball-to-powder weight ratio of 10:1. The jar was placed in a rotation device, and the mixing was made with a constant rotation speed of 40 rpm, during 6 days (low-energy ball milling).	<b>HUP:</b> Uniaxial load pressure of 35MPa and a temperature of 550°C during 10min.	2 wt% 4 wt% 6 wt%	XXX
Chen et al. (2016) [23]	<b>Ball milling:</b> Al powder is milled with 2 wt.% stearic acid. The powder is sealed in a ZrO <sub>2</sub> jar together with 600 g ZrO <sub>2</sub> media balls (10mm in diameter) in an argon gas atmosphere. The rotation speed is 200 for 240 min. Then, Al-flake powder	<b>SPS and hot extrusion:</b> Sintering at 800 K, 850 K and 900 K. The heating rate is 20 K/min and the holding time at target temperatures is 60min. A pressure of 30MPa is applied on the sample under a vacuum of ~5 Pa. Before	1 wt%	>99%

Reference	Blending method	Sintering method	CNT content Value wt%	Relative density Value %
	is mechanically bathed in isopropyl alcohol-based solution with ~1 wt.% zwitterionic surfactants and 1 wt.% CNTs in a plastic bottle on a rocking ball milling machine for 120 min. Thirty-gram ZrO <sub>2</sub> media balls were added to assist the coating of CNTs on flaky powders.	hot extrusion, the sintered sample is preheated to 700 K and kept for 180 s under an argon gas atmosphere. Then, the billet is immediately put into a steel container) and extruded through a die. The extrusion ratio and the ram speed are 37:1 and 3mm/s, respectively.		

**Table 1.** Summary of blending and sintering methods for the production of Al/CNT composites.

**2.2. Distribution and interaction with the matrix material**

In all the analysed articles, CNT agglomeration is observed, being the size and amount of those agglomerates strongly related to the chosen dispersion method. Specifically, in those reports where ball milling is used, a significant clustering is noticed. This might be due to the use of non-functionalized CNTs that tend to easily re-agglomerate during processing. Yet, the utilization of functionalized CNTs in ball milling mixed blends would not bring any further improvement, since the structural quality of the CNTs would be significantly lower. However, despite the presence of unavoidable agglomerates, very fine cluster dispersion and a homogeneous distribution can be observed. Interestingly, one would assume that the formation of clusters would be detrimental to the proper densification of the composites. However, as already depicted in Table 1, the final densities of the composites were never below 94%. The formation of clusters is one of the most challenging problems to overcome when dealing with CNTs, since a trade-off between an optimal initial agglomerate disentanglement and the lowest possible damage to the CNT structural state must be found. There are two ways to observe the amount of agglomerates in the composites. Certain reports focus on the evaluation by electron microscopy on the polished surface of the samples, whereas other authors evaluate fracture surfaces of the composites. Both approaches are valid, in the sense that they show a good overview of the agglomeration. However, SEM imaging of the surface would allow a further quantification of the agglomerates size and distribution by segmenting the C-containing phases. Bakshi proposed an interesting methodology to quantify the dispersion, based on distance calculation algorithms from electron micrographs, which can be found in **Bakshi et al.** [93].

If we focus our attention on the CNT degradation during blending and after densification, we observe dissimilar results obtained by Raman spectroscopy, even for the same manufacturing method. For example, in samples densified by SPS (a technique known to exert strong thermomechanical stress on the CNTs), negligible variation of the  $I_D/I_G$  ratio is reported [23,79]

as opposed to an increase in the defect density in other reports [18]. It is therefore very difficult to discern whether the sintering process has indeed any sort of influence on the CNT degradation. It has been already reported that given the strong stresses from SPS, CNTs are usually either damaged or degraded within the matrix material [94]. When strong shear forces are applied as in the case of HPT, sharp increases in the D band intensity are measured, depicting a modification of the graphitic structure. In all cases, an increased amount of structural damage would favour the reactivity of the CNT shells.

The CNT degradation is a major issue when working with metals which are strong carbide builders [95]. It is well known that aluminium tends to form a stable carbide ( $\text{Al}_4\text{C}_3$ ) in a wide compositional range [96], being of brittle nature and having the major drawback of being water soluble [97]. Some authors mention that the formation of this carbide would not be as detrimental as expected [18,58], since it only sacrifices the outermost CNT layer, providing an optimal interface with the matrix. However, despite being able to efficiently transfer the applied load, the utilization of the composite in structural applications in humid environments would lead to an interfacial degradation. Another way to obtain this carbide is by transitioning from  $\text{Al}_2\text{O}_3$  to  $\text{Al}_4\text{C}_3$  [98]. Yet, this phase transition occurs only under certain circumstances that are rarely achieved in solid-state processing.

### 3. Copper/CNT system

#### 3.1. Solid-state processing

Reports on the solid-state processing of Cu/CNT systems deal with a variety of different raw materials, blending methods and sintering techniques, therefore sticking out in the research field of CNT-reinforced metal matrix composites.

When it comes to the used Cu starting material, a great many of commercially available powders or chemicals are employed, making it very hard to compare the Cu/CNT systems of different publications. The materials used depend directly on the blending and production process that has been used. The range goes from nanosized to almost 100  $\mu\text{m}$  sized Cu powder particles, having different particle shapes (spherical, dendritic) and various purity grades between >99.5% and >99.95% [6–12,14,15,32–35,42–44,50,52–55,63–71]. The most used blending methods are ball milling, molecular-level mixing or colloidal mixing, each having their advantages and disadvantages as discussed in the introduction [6–12,14–17,32–35,42–45,51–55,63–75]. But especially for Cu, molecular-level mixing is employed very often, using copper compounds in solvents that have to be chemically treated in order to become pure copper (e.g. copper(II) acetate monohydrate, Cu(II) sulphate pentahydrate or simply CuO). Some prominent suppliers for the Cu starting materials are Sigma-Aldrich (USA), Alfa Aesar GmbH & Co. KG (Germany), Chang Sung Co. (Korea), Junsei Chemical Co. Ltd (Japan), Kojundo Chemical Lab. Co. Ltd (Japan), TLS Technik GmbH (Germany) or New Materials Research Co. Ltd (China) [6,12,14–16,32,33,42,54].



Therefore, to review the progress in Cu/CNT composites, a detailed comparison of blending methods, sintering techniques and achieved final relative composite densities has to be conducted, which can be found in **Table 2**.

Reference	Blending method	Sintering method	CNT content	Relative density
Tu et al. (2001) [63]	<b>Ball milling:</b> CNTs are milled for 8 h in an organic liquid. Then, CNTs are sensitized, activated and finally coated by electroless nickel. Copper- and nickel-coated CNTs are mixed for 30 min in a ball mill.	<b>CPS:</b> Isostatically pressed at a pressure of 600 MPa at 100 °C for 10 min under vacuum. Then sintered at 800 °C for 2 h.	4 vol%	97.5%
			8 vol%	97.5%
			12 vol%	97% 95%
			16 vol%	
Chen et al. (2003) [35]	<b>Ball milling:</b> CNTs are sensitized, activated and then coated by electroless nickel for 15 min. Then, copper powder and nickel-coated CNTs are mixed by ball milling for 30 min.	<b>CPS:</b> Isostatically pressed at a pressure of 600 MPa at 100 °C for 10 min under vacuum. Then sintered at 800 °C for 2 h.	4 vol%	97.5%
			8 vol%	97.5%
			12 vol%	97% 95%
			16 vol%	
Kim et al. (2006) [64]	<b>Ball milling:</b> Cu powder and CNTs are mixed through high energy ball milling process for 24h with 150rpm.	<b>SPS and cold rolling:</b> Pre-compacted under a pressure of 10 MPa and then sintered at 700 °C for 1 min in vacuum (0.13 Pa) under a pressure of 50 MPa with a heating rate of 100 °C/min. Finally, the samples are cold rolled up to 50% reduction, followed by full annealing at 650 °C for 3 h.	5 vol%	99.3%
			10 vol%	99.1%
Kim et al. (2007) [51]	<b>Molecular-level mixing process:</b> CNTs are purified and functionalized by acid treatment. Then, Cu acetate monohydrate is added and sonicated for 2h. The solution is vaporized with magnetic	<b>SPS:</b> Sintered at 550°C for 1 min in vacuum( 0.1 Pa) with a pressure of 50MPa and a heating rate of 100 K/min.	5 vol%	99% 99%
			10 vol%	

Reference	Blending method	Sintering method	CNT content	Relative density
	stirring at 100 °C, followed by calcination at 350 °C in air. and reduction under N <sub>2</sub> atmosphere.			
Kim et al. (2008) [9]	<b>Molecular-level mixing process:</b> CNTs were purified under sonication for 10 hours and then functionalized. Then, 20 mg of CNTs are sonicated in 300ml ethanol for 2 hours. Cu(CH <sub>3</sub> COO)•2 H <sub>2</sub> O is added and sonicated again for 2 hours. After drying at 250 °C in air and calcinating at 300 °C in air, the powder is reduced under a hydrogen atmosphere.	<b>SPS:</b> Pre-compacted under a pressure of 10 MPa and then sintered at 550°C for 1 minute in vacuum (0.13 Pa) with a pressure of 50 MPa. The heating rate is 100°C/ min.	5 vol% 10 vol%	98 ± 2% 98 ± 1.5%
Kim et al. (2008) [11]	<b>Molecular-level mixing process:</b> CNTs are cleaned and functionalized. Then, 10.5 mg of CNTs are dispersed in 100 ml of oleylamine in an ultrasonic bath for 3 h. 3 g of copper acetate monohydrate is added and the solution is purged with argon for 1 h. Then, the mixture is heated to 523 K for 10 min with a heating rate of 10 K/min. After cooling, the powders are reduced at 573 K for 2 h under hydrogen atmosphere.	<b>SPS:</b> Sintering at 823 K for 1 min in vacuum (0.13 Pa) with a pressure of 50 MPa and a heating rate of 100 K/min.	5 vol%	XXX
Daoush (2008) [12]	<b>Molecular-level mixing process:</b>	<b>SPS:</b> Sintered at 600°C	10 vol%	97.9%
	Copper (II) sulphate pentahydrate,	for 1 min with a pressure of	20 vol%	97% 96.
	tri-sodium citrate monohydrate	20 MPa under vacuum	30 vol%	7% 96%
	and CNTs are stirred with 500 rpm magnetic stirrer	(0.13 Pa).	40 vol%	

Reference	Blending method	Sintering method	CNT content	Relative density
	for 2 h at room temperature to suspend the CNTs in the solution. The equivalent formaldehyde amount is added with a rate of 0.1 ml/min within 30 min. The solution is filtered, washed and vacuum dried at 100°C for 2 h and finally reduced at 400°C for 30 min under hydrogen atmosphere.			
<b>Chai et al. (2008) [15]</b>	<b>Particle Composite System mixing:</b> CNTs are cleaned in nitric acid in the ultrasonic bath. Mixing condition is 5000 rpm in rotary speed for 40 min.	<b>SPS:</b> Sintered at 600 °C for 5 min. The heating rate is 100 °C/min and a pressure of 50 MPa is applied.	5 vol% 10 vol% 15 vol%	98.4% 98.6% 96.1%
<b>Li et al. (2009) [65]</b>	<b>Ball milling:</b> In an argon protected environment at room temperature. The mass ratio of ball to powder is 10:1, and the milling time is 5 h.	<b>HPT:</b> Pre-compacted with 500 MPa in air at room temperature. Then consolidated under 6 GPa for 5 revolutions at room temperature.	1 wt%	XXX
<b>Li et al. (2009) [66]</b>	<b>Ball milling:</b> In an argon protected environment for 5 h	<b>HPT:</b> Pre-compacted and then consolidated under 6 GPa for 5 revolutions at room temperature.	1 wt%	XXX
<b>Chu et al. (2010) [55]</b>	<b>Particle Composite System mixing:</b> CNTs are purified in nitric acid in an ultrasonic bath, then filtered, washed and dried at 120°C. The mixing is performed with 5,000 rpm for 40 min.	<b>SPS:</b> Sintered at 550°C-650°C in vacuum (<5 Pa) with a pressure of 40-60 MPa for 5-10 min. The heating rate is 100°C/ min.	5 vol% 10 vol%	96.2% - 99.2% 95.3% - 98.9%
<b>Cho et al. (2010) [42]</b>	<b>Colloidal mixing process:</b> CNTs are sonicated in acid solution at 323 K for 24h. Then, Cu powder and CNTs were sonicated separately in ethanol solution for 1 h,	<b>SPS:</b> Sintered at 823 K for 1 min under a uniaxial pressure of 50 MPa. The heating rate is 50 K/min.	0.5 vol% 1 vol% 1.5 vol% 2 vol% 3 vol% 5 Vol%	96.8 - 99.0%

Reference	Blending method	Sintering method	CNT content	Relative density
	blended, stirred for 30 min and oven-dried at 323 K. The powders are finally heat-treated at 623 K for 1 h in Ar-5% H <sub>2</sub> atmosphere.		10 vol%	
Uddin et al. (2010) [67]	<b>Ball milling:</b> Milled in Ar atmosphere and for different hours with 50 stainless steel balls (diameter of each ball: 10 mm, ball to powder ratio 10:1, milling speed: 200 rpm). For bronze composites, the chemical composition is Cu 79%, Sn 10%, Zn 3% and Ni 8%.	<b>HUP:</b> Sintering at 750 °C with pressure of 40 MPa for Cu-CNT composites in Ar-atmosphere, whereas 800 °C and 40 MPa for Bronze-CNT composites.	Cu 0.1 wt% Cu	96.8%
			0.5 wt% Cu	96.8%
			Cu 1 wt% Cu	91%
			2 wt% Cu	82.6%
			4 wt% Cu	95.9%
			wt% Cu	93.8%
			Bronze	88.9%
			0.1 wt% Bronze	89.9%
			0.5 wt% Bronze	85.6%
			1 wt% Bronze	
			2 wt% Bronze	
			4 wt% Bronze	
Xu et al. (2011) [8]	<b>Ball milling:</b> Milled for 5 h in an organic liquid.	<b>CPS:</b> Cold pressed at 200 MPa, then sintered at 850 °C in vacuum atmosphere for 5 h. After cooling, a second pressing at 600 MPa and a second sintering are performed.	10 vol%	96%
Jenei et al. (2011) [33]	<b>Ball milling</b>	<b>HPT:</b> Pre-compacted by cold pressing. Then consolidated at RT and 373 K with a pressure of 2.5 GPa and 10 revolutions.	3 vol%	97%
Kim et al. (2011) [52]	<b>Molecular-level mixing process:</b> CNTs are cleaned and functionalized. Then, the CNTs are dispersed within ethanol by sonication. Cu (CH <sub>3</sub> -COO)•2H <sub>2</sub> O is added to	<b>SPS:</b> Sintered at 823 K f	5 vol%	XXX
		<b>CPS:</b> Pre-compacted using a hydraulic press 130 kN. Then sintered in a tube furnace at 600 °C in vacuum (10.6 Pa) or 1 min in vacuum (0.13 Pa) with a	10 vol%	

Reference	Blending method	Sintering method	CNT content	Relative density
	the CNT suspension and sonicated for 2 h. After vaporization at 333–373 K and calcination at 573 K in air, the powders are reduced at 523 K for 4 h under hydrogen atmosphere.	pressure of 50 MPa.		
Rajkumar et al. (2011) [43]	<b>Colloidal mixing process:</b> CNTs are purified and oxidized using nitric acid treatment by sonication for 10 min at 60°C. Then, the CNTs are sensitized and activated. The activated CNTs are introduced into the electroless copper bath and stirred for 30 min while using sonication. The coated CNTs are dispersed in ethanol with vigorous sonication for 10 min after which the copper powder is added. The solution is stirred and evaporated at 120°C. The powder is finally mixed in an electric agate pestle mortar for 2 h.	<b>Microwave Sintering:</b> Pre-compacted in a hydraulic press. Sintering at 800°C with the soaking time of 5 min with a ramp rate of 12 °C/min.	5 vol%	95.5%
			10 vol%	96%
			15 vol%	96.5%
			20 vol%	94%
Guiderdoni et al. (2011) [44]	<b>Colloidal mixing process:</b> CNTs are dispersed in deionized water using a sonotrode for a few seconds. The Cu powder is added. After further sonication of 1 min, the dispersion is immersed in liquid N <sub>2</sub> for 2 min and freeze-dried at -40 °C for 48 h in vacuum (12 Pa).	<b>SPS:</b> Sintered in vacuum (<10 Pa) at 700°C with a heating rate of 100 °C/min for 6 min. The pressure of 100 MPa is gradually applied within the first minute of the dwell and maintained during the remaining 5 min. Samples are naturally cooled.	0.5 vol%	95% 96%
			1 vol%	98% 96%
			2 vol%	93% 93%
			3 vol%	88% 78%
			4 vol%	
Pham et al. (2011) [34]	<b>Ball milling:</b> The CNTs are treated in acid at 60 °C for 4 h. Then, the CNTs are dispersed in acetone. The Cu powder and the CNTs dispersed in acetone are mixed through a	<b>CPS:</b> Sintering at temperatures of 850, 900 and 950° C for 2 h in argon atmosphere.	0.5 wt%	XXX
			1 wt%	
			1.5 wt%	
			2 wt%	
			2.5 wt%	
			3 wt%	



Reference	Blending method	Sintering method	CNT content	Relative density
	high-energy ball milling process for 6 h at 300 rpm.		3.5 wt%	
Firkowska et al. (2011) [14]	<b>Molecular-level mixing process:</b> CNTs are functionalized by polymer wrapping and dispersed in 1 wt% Poly(sodium 4-styrenesulfonate) by sonication for 2 h and stirring overnight. Then, CNTs are oxidized, washed and suspended in water by ultrasonic treatment. Copper acetate is added. After 12 h, the suspension is heated up to 70 °C to evaporate the solvent. After calcination, the mixture is finally reduced under H <sub>2</sub> at 350 °C for 2 h	<b>CPS:</b> Pre-compacted using a hydraulic press 130 kN. Then sintered in a tube furnace at 600 °C in vacuum (10.6 Pa) for 60 minutes. <b>SPS:</b> Pre-compacted under a pressure of 6 kN. Then sintered at 600 °C for 5 min in a vacuum a pressure of 50 MPa and a heating rate of 100 °C/min.	0.2 wt% 1 wt% 3 wt% 10 wt%	XXX
Xue et al. (2012) [7]	<b>Molecular-level mixing process:</b> Dispersion of CNT in ethanol (1 g/l) by sonication for 30 min. Cu(CH <sub>3</sub> COO)•2H <sub>2</sub> O (2g/ml) is dissolved in NH <sub>3</sub> •H <sub>2</sub> O (40%), mixed and sonicated for 30 min with the CNT dispersion. After solvent vaporization and calcination, the powder is reduced at 250 °C for 2 h under hydrogen atmosphere.	<b>SPS and hot rolling:</b> At 550 °C (vacuum 0.1 Pa) under a pressure of 50 MPa for 5 min with a heating rate of 100 °C/min. Then hot rolled up to 50% reduction at 650 °C.	5 vol%	XXX
Shukla et al. (2012) [10]	<b>Ball milling:</b> Using stainless steel balls of Ø 3/8 inch (ball to powder ratio 5:1) under argon with 200 rpm for 20h.	<b>HUP:</b> Sintering at 700 °C with 30 MPa pressure under vacuum (0.001 Pa) for 30 minutes.	5 vol%	93.4%
Chu et al. (2013) [68]	<b>Ball milling:</b> Mixed with Cu–Ti powders with 1200 rpm for 2h. Ball-to-powder weight ratio is 10:1. Alcohol is added.	<b>HUP:</b> At 760 °C for 20 min under an uniaxial pressure of 40 MPa	5 vol% 10 vol% 15 vol%	99% 98% 96%
Guiderdoni et al. (2013)	<b>Colloidal mixing process:</b> CNTs are dispersed in deionized	<b>SPS:</b> At 700°C (vacuum <10 Pa) under a pressure of 100	5 vol% 8,4 vol%	96% 85% 82% 73%

Reference	Blending method	Sintering method	CNT content	Relative density
[6]	water using a sonotrode (a few seconds). Cu powder is then added and sonicated for one minute. The dispersion is immersed in liquid N <sub>2</sub> for 2 min and freeze-dried at -40 °C for 48 h in vacuum (12 Pa).	MPa for 6 min with a heating rate of 100 °C/min. Then natural cooling.	17,1 vol% 33,2 vol%	
Jenei et al. (2013) [32]	<b>Ball milling</b>	<b>HPT:</b> Pre-compacted by cold pressing and consolidated at RT and 373 K with 2.5 GPa and 10 revolutions.	3 vol%	97%
Lal et al. (2013) [53]	<b>Molecular-level mixing process and Ball milling:</b> CNTs are functionalized in acidic solution. After washing and drying, they are dispersed in Sodium dodecyl sulphate (SDS). And coated with copper. Copper powder is ball milled for 10 h at 500 rpm using stainless steel balls (5 mm). Ball to powder ratio is 10:1 and ethanol is taken as a process control reagent. Copper-coated CNTs are milled together with previously milled Cu powder for 5 h at 250 rpm.	<b>CPS:</b> Pre-compacting with 500 MPa pressure. Then sintering at 900°C for 4 h under vacuum (1.33 Pa).	0.5 wt% 1 wt% 1.5 wt%	XXX
Tsai et al. (2013) [54]	<b>Molecular-level mixing process:</b> CNTs are functionalized and treated with 250 ml of oleylamine at room temperature for 2.5 h. 3 g of copper (II) acetate monohydrate are added and the mixture is sealed and purged in an argon-protected environment for 4 h. After heating to 523 K with 10K/min for 15 min, the powder is cooled, calcinated at 573 K in air for 2 h and then reduced in a N <sub>2</sub> atmosphere.	<b>HPT:</b> Rotation speed of 1 rpm with a load of 2.5 GPa at room temperature for 5 revolutions. The rotation is initiated 5 s after the load application.	5 vol%	XXX

Reference	Blending method	Sintering method	CNT content	Relative density
Shukla et al. (2013) [69]	<b>Ball milling:</b> Using stainless steel balls of 10 mm diameter (ball to powder ratio 5:1) under argon atmosphere at 200 rpm for 20 h.	<b>HUP:</b> Sintering at 700°C for 30 min using 30 MPa uniaxial stress under vacuum (0.001 Pa). The compacts produced underwent delamination in the centre on cooling and were repressed at 725°C under same conditions.	0.2 vol% SWCNT 5 vol% SWCNT 10 vol% S WCNT 5 vol% MWCNT 10 vol% MWCNT	95% 99% 97% 96% 98%
Chu et al. (2013) [70]	<b>Ball milling:</b> Mixed with Cu-0.76wt.% Cr alloying powder under argon atmosphere with a rotary speed of 1200 rpm for 120 min. A ball-to-powder weight ratio of 10:1 is used, and alcohol is added.	<b>HUP:</b> Pre-compacted to a green density of 75% and then consolidated at 750 °C for 15 min with a heating rate of 50 °C/min and a pressure of 40 MPa .	5 vol% 10 vol% 15 vol%	XXX
Yoon et al. (2013) [71]	<b>Ball milling:</b> Using stainless steel balls for 1 h (ball-to-powder weight ratio was 15:1) and 15 rpm.	<b>HPT:</b> Under room temperature and 6 GPa using 10 revolutions at a constant speed of 1 rpm.	5 vol% 10 vol%	99% 99%
Sule et al. (2014) [45]	<b>Colloidal mixing process:</b> Copper powder and CNTs are dispersed separately in 60 ml ethanol using sonication. CNTs were sonicated for 1 h, stirred for 5 min, sonicated again for 30 min and stirred again for 3 min. Copper powder is sonicated in ethanol for 1 h and stirred for 2 min. The slurries are mixed together, sonicated for 1 h and stirred for 3 min. After drying using a rotary evaporator, the powder is annealed for 30 min at 550 °C with a heating rate of 5 °C/min under inert Ar atmosphere to reduce the oxygen content.	<b>SPS:</b> Sintered at 650°C under a vacuum of 1 hPa. A constant pulse-to-pause ratio of 10:5 (10 ms on and 5 ms off) is applied under a pressure of 50 MPa.	1 vol%	97%
Barzegar Vishlaghi	<b>Ball milling:</b> CNTs are sonicated in acetone for 20	XXX	XXX	XXX

Reference	Blending method	Sintering method	CNT content	Relative density
(2014) [72]	and cleaned in nitric acid for 1 h. Cu and Fe powder is milled for 15h. Then, CNTs are added and milled a gain for 15h using chromium steel balls under argon atmosphere with 300 rpm and a ball to powder weight ratio of 20:1.			
Imai et al. (2014) [75]	<b>Dipping process:</b> Dipping Cu <sub>0.5</sub> Ti powder into a zwitterionic surfactant water solution (3-(N,N-dimethyl stearyl ammonio) propanesulfonate) with CNTs. The powders are then dried at 353 K for 7200 s in air. To remove surfactant films, powders are heated to 873K in H <sub>2</sub> and Ar atmosphere.	<b>SPS:</b> Sintered at 1223 K for 1800 s under 30 MPa in vacuum (6 Pa). The compacts are preheated at 1073K for 800s with a heating rate of 1K/s in Ar atmosphere. After preheating, immediately extruded by using hydraulic press under an extrusion ratio of 12.8.	0.19 wt% 0.34 wt%	XXX
Akbarpour et al. (2015) [73]	<b>Ball milling:</b> In Ar atmosphere for 3 h at 200 rpm using 10 mm balls, with a 10:1 ball to powder weight ratio and 0.5 wt% of stearic acid.	<b>HPT:</b> Pre-consolidated at a load of 150 MPa and a temperature of 973 K with a holding time of 30 min. Then, HPT process at room temperature with 6 GPa and various numbers of revolutions.	4 vol%	99.6%
Chen et al. (2015) [17]	<b>Ball milling:</b> The CNT and NbSe <sub>2</sub> are coated with copper by electroless plating. CNTs and NbSe <sub>2</sub> are mixed with Cu powder mechanically.	<b>CPS:</b> Powders are cold pressed with 200 MPa and sintered at 750 °C for 2 h in N <sub>2</sub> shielding. The sintered compact is crushed, repressed at 400 MPa and sintered again at 750 °C for 2 h in N <sub>2</sub> shielding.	1-4 vol% CNT with various amounts of copper-coated NbSe <sub>2</sub>	XXX
Sule et al. (2015) [16]	<b>Colloidal mixing process:</b> CNTs are sonicated in ethanol for 1 h and stirred for 5 min using a magnetic stirrer. Then, Ru powder is added, combined with further sonication for 1 h	<b>SPS:</b> Sintering at 600 or 650°C with a heating rate of 80°C/min, a holding time of 5 min and a pressure of 50 MPa.	1 vol% CNT (600°C) 2 vol% CNT (600°C)	98.28% 98.15% 97.72% 96.77% 96.15% 97.63%

Reference	Blending method	Sintering method	CNT content	Relative density
	and stirring for 3 min. Copper powder was ultrasonicated in ethanol for 1 h and stirred for 2 min. The slurries are mixed together and are sonicated for 1 h and stirred for 3 min. After drying, the powders are further blended in a Turbula T2F mixer for 1h at a speed of 101 revolutions per minute and finally annealed for 30 min at 550 °C with a heating rate of 5 °C/min under inert Ar atmosphere to reduce the oxygen content.		0.5 vol% CNT 0.5 vol% Ru (600°C) 1 vol% CNT 0.5 vol% Ru (600°C) 2 vol% CNT 0.5 vol% Ru (600°C) 1 vol% CNT 0.5 vol% Ru (650°C) 2 vol% CNT 0.5 vol% Ru (650°C)	97.08%
Varo et al. (2015) [74]	<b>Ball milling:</b> Flake Cu–CNT nanocomposite powders are synthesized by 5h of ball milling, using a rotation speed of 300rpm; the ball-to-powder ratio is 5:1.	<b>CPS:</b> Pre-compacted with 200 MPa of uniaxial pressure at room temperature. Then, the green pellet is warm-pressed at 500 MPa for 1 h at 500°C and finally sintered in a tube furnace at 950°C for 2 h under argon atmosphere.	0.5 wt% 1 wt% 0.15 wt% 0.2 wt% 0.25 wt% 3 wt% 5 wt%	Decreasing density with increasing CNT content.

**Table 2.** Summary of blending and sintering methods for the production of Cu/CNT composites.

### 3.2. Distribution and interaction with the matrix material

The only stable copper carbide known is the copper acetylide  $\text{Cu}_2\text{C}_2$  [99]. It is usually observed as a transition phase during the purification of Cu and after the reaction of cuprous oxide with water [99]. In the studied Cu-CNT composites, no carbide was detected whatsoever. However,



in certain cases, CuO and Cu<sub>2</sub>O were observed as a result of the selected manufacturing process. This issue is overcome by utilizing reagents (such as EDTA) or a reducing atmosphere as a post-processing method.

Regarding interfacial features, there is a publication that reported on the influence of adsorbed oxygen on the CNT surface on the interfacial strength, observing an improved interface but a reduction in the transport properties [14]. Theoretical simulations have demonstrated that the addition of oxygen-containing functional groups results in improved interfaces. The assertion is based on the fact that chemically active oxygen on CNT surfaces might improve the binding of metals with CNTs by enhancing the electron exchange between the metal and the carbon atoms or by directly interacting with the metal [100].

In some cases, the presence of alloying elements in the matrix degraded the CNTs into carbides as for example: the presence of Al leads to the formation of Al<sub>4</sub>C<sub>3</sub> [50], and the presence of Cr leads to the formation of Cr<sub>3</sub>C<sub>2</sub> [70]. Another approach was considered by mixing the CNTs with a Cu-Ti alloy. Chu et al. showed that the CNTs reacted in the presence of Ti, resulting in a degradation of the CNTs into a TiC interphase, despite having only 0.85 wt% Ti in the mixture [68]. This reaction between the CNTs and the carbide forming alloying elements is usually referred to as an interfacial improvement, leaving aside the fact that the CNTs are likely degraded into a hardly improving second phase in the composites.

On the other side, there are reports in which a seamless interface was achieved even avoiding any phase formation, as shown by Cho et al. [42]. This coherent interface would then result in the reduction of detrimental features such as thermal resistance.

In certain cases, XRD is used to observe the possible interphase formation; however, it would not be sufficient to resolve it since the volume fraction of the formed phases would be low. HR-TEM is the most suitable way to characterize these interphases with the aid of SAED.

A very interesting way to overcome the reaction between the CNTs and the alloying elements was addressed by decorating the CNTs with Cu nanoparticles [14,43]. In this case, a good distribution was achieved, rendering improvements in hardness and thermal resistance, despite reducing the CNTs intrinsic properties.

The analysis of the agglomeration and distribution of CNTs was, in all cases, qualitatively reported. As a general case, the CNT distribution was acceptable, with low reagglomeration activity. Both, the reaction with alloying elements as well as the covalent functionalization of the CNTs (as in MLM) tends to reduce significantly the intrinsic properties of the nanotubes, thus hindering an optimal exploitation of the CNT usage.

Regarding the adhesion of the reinforcement to the matrix, the best outcomes are observed when covalent functionalization is used (MLM) or an interphase is formed. In the case of non-functionalized CNTs, the adhesion to the matrix is poor, mainly due to a poor metal-CNT wettability [95].

## 4. Nickel/CNT system

### 4.1. Solid-state processing

For Ni/CNT, as for the other composite materials, there is a large variety of starting materials that have been used to fabricate the composites. Suppliers that are found very frequent for Ni powders are Alfa Aesar (Germany) and Crucible research (USA) [26–31,36–38,47,76,78,80]. The range of used powders reaches from 120 nm up to 149 µm in particle size, having a dendritic or spherical morphology and showing a purity of 99.8% to 99.99% [24–31,36–38,46–49,76,78,80]. The most used blending method for Ni/CNT composites is colloidal mixing and ball milling [24,26–31,36,38,46–49].

A detailed overview of the research papers in the Ni/CNT composite manufacturing can be found in **Table 3**.

Reference	Blending method	Sintering method	CNT content	Relative density
Yamanaka et al. (2007) [46]	<b>Colloidal mixing process:</b> Stirred with an ultrasonic homogenizer and a scroller is used as a means to obtain a homogenous mixture. The slurry is dried for 24 h using a porous Al <sub>2</sub> O <sub>3</sub> board.	<b>SPS:</b> Heating and cooling rate of 50K/min with a holding time of 1min. Sintered within the range of 673–1073 K. The sintering pressure is 50 MPa in vacuum (<5 Pa).	1 vol%	80% 94%
			(673 K)	97% 97%
			1 vol%	99% 99.5%
			(773 K)	99.5%
			1 vol%	99.9%
			(873 K)	98.3%
			1 vol%	97.5%
			(973 K)	
			1 vol%	
			(1073 K)	
			2 vol%	
Hwang et al. (2008) [76]	<b>Roller mixing:</b> Mixed in a twin-roller mixer consisting of two rolls rotating in opposite directions (one clockwise and one anticlockwise). This mixing is carried	LENS	(1073 K)	
			2 vol%	
			(1073 K)	
			3 vol%	
			(1073 K)	
			4 vol%	
			(1073 K)	
			5 vol%	
			(1073 K)	
			10 vol%	
			(1073 K)	
			10 vol%	XXX

Reference	Blending method	Sintering method	CNT content	Relative density
	out for 24 h.			
Scharf et al. (2009) [37]	<b>Roller mixing:</b> Mixed in a twin-roller mixer consisting of two rolls rotating in opposite directions (one clockwise and one anticlockwise). This mixing is carried out for 24 h.	<b>LENS:</b> Pulsed Nd:Yttrium aluminium garnet laser (power rating of 500 W, wavelength of 1.064 nm) is focused on the substrate to create a melt pool into which the powder feedstock is delivered through Ar gas (mass flow rate 3.5 l/min). Laser power of 400 W, 35 A current, hatch width of 6.35 mm, layer thickness of 0.01 in.	10 vol%	XXX
Hwang et al. (2009) [36]	<b>Ball milling:</b> For 48 hours using two different sizes of tungsten carbide balls of diameter 12.7 and 6.35 mm.	<b>LENS:</b> Pulsed Nd:YAG laser (power rating of 500 W, wavelength of 1.064 nm) is focused on the substrate to create a melt pool into which the powder feedstock is delivered through Ar gas. Laser power of 300 W, 30 A current.	5 wt%	XXX
Singh et al. (2010) [38]	<b>Ball milling:</b> For 48 hours using two different sizes of tungsten carbide balls of diameter 12.7 and 6.35 mm.	<b>LENS:</b> Pulsed Nd:YAG laser (power rating of 500 W, wavelength of 1.064 nm) is focused on the substrate to create a melt pool into which the powder feedstock is delivered through Ar gas.	15 vol%	XXX
Suárez et al. (2012) [47]	<b>Colloidal mixing process:</b> Merging of the dispersion of the CNTs in an ultrasound bath with N,N-dimethylformamide (DMF) and the subsequent addition of Ni powder. The CNT concentration is 0.023 mg/ml. After 10min in the ultrasound bath, the resulting solution was stirred to homogenize the mixture and then dried in a ventilated furnace. The powder is finally	<b>CPS and HUP:</b> Uniaxially pressed with a pressure of 990 MPa. Then sintered in a vacuum (2 Pa) tube furnace at 950°C for 2.5 h. Or sintered in a hot uniaxial press in vacuum (0.2 Pa) at 750°C for 2.5h with an axial pressure of 264MPa.	1 wt%	93.7% (CPS) 95.5% (HUP)

Reference	Blending method	Sintering method	CNT content	Relative density
	milled in an agate mortar.			
Hwang et al. (2013) [25]	<b>Molecular-level mixing process:</b> CNTs were purified and functionalized by using HF, acid solution mixture of H <sub>2</sub> SO <sub>4</sub> /HNO <sub>3</sub> . After cleaning and drying, they are dispersed in ethylene glycol solution by ultra-sonication and Ni(C <sub>2</sub> H <sub>3</sub> O <sub>2</sub> ) <sub>2</sub> •4H <sub>2</sub> O is added. Then 2 M-NaOH and hydrazine are injected into the mixed solution, heated to 70 °C and kept 30 min. Finally, the reduction process of fabricated CNT/Ni composite powders is performed in H <sub>2</sub> + CO mixed atmosphere for 2 h at 400°C.	<b>SPS:</b> Pre-compacted under a pressure of 10 MPa. Sintered at 700 °C for 1 min under vacuum (0.13 Pa) employing a pressure of 50 MPa. The heating rate is maintained at 100 °C/ min.	6 vol%	98-99%
Suárez et al. (2013) [78]	XXX	<b>CPS:</b> Manufactured by cold pressing at 990 MPa and sintering at 950 °C for 2.5 h in vacuum. .	1 wt% 3 wt% 5 wt%	95-96%
Suárez et al. (2013) [26]	<b>.Colloidal mixing process:</b> Merging of the dispersion of the CNTs in an ultrasound bath with ethylene glycol and the subsequent addition of Ni powder. The CNT concentration is 0.2 mg/ml. After 10min in the ultrasound bath, the resulting solution was stirred to homogenize the mixture and then dried in a ventilated furnace. The powder is finally milled in an agate mortar.	<b>HUP:</b> Cold pressed with 990 MPa. Then sintered in a hot uniaxial press under vacuum (0.2 Pa) at 750 °C for 2.5 h with a 264MPa axial pressure.	1 wt% 2 wt% 3 wt% 5 wt%	95-97%
Sairam et al. (2014) [80]	No mixing, only pure Ni (high purity 99.99%) with a size range from 1 to 5 µm.	<b>SPS:</b> Pre-compacted under a pressure of 5 MPa. Then sintered at 700, 850 or 1000 °C for 5 min under a controlled argon atmosphere under a	XXX	96.8-97.7% (700°C) 97.8-99% (850°C)

Reference	Blending method	Sintering method	CNT content	Relative density
		pressure of 50, 65 or 80 MPa. The heating rate is maintained at 100°C/min.		98.1 -99.2% (1000°C)
<b>Borkar et al. (2014) [24]</b>	<b>Ball milling or molecular-level mixing:</b> High energy ball milling for 24 h at 400 rpm. For the MLM process, CNTs are purified and functionalized by acid treatment. After cleaning and drying, they are dispersed in ethylene glycol by ultra-sonication and $\text{Ni}(\text{C}_2\text{H}_3\text{O}_{22}) \cdot 4\text{H}_2\text{O}$ is added. Then, 2 M-NaOH and hydrazine are injected, the solution is heated to 70 °C and kept 30 min. Finally, the CNT/Ni composite powders are reduced in $\text{H}_2$ + CO mixed atmosphere for 2 h at 400°C.	<b>SPS:</b> Pre-compacted under a pressure of 5 MPa. Then sintered at 800 °C for 5 min under controlled argon atmosphere under a pressure of 80 MPa. The heating rate is maintained at 100° C/min.	5 vol%	XXX
<b>Nguyen et al. (2014) [48]</b>	<b>Colloidal mixing process:</b> Functionalization of the metal powders and CNTs by zwitter-ionic surfactant, 3-(N,N-dimethylstearylammonio)- propane-sulfonate (ZW). Suspensions with varying concentration of ZW (0.04-0.10 wt%) in de-ionized water are heated to 353 K for 10 min with a fixed CNT concentration (0.1 wt%) and ultrasonicated for 15 min. The metal powder is submersed in 100 ml of the 0.06 wt% ZW-0.1 wt% CNT suspensions with varying amounts of dwell time from 1 to 6 h. The ZW-CNT-metal powder suspensions are then dried at 423 K in vacuum, and the dried powders are subsequently annealed in a vacuum	<b>SPS:</b> Consolidated at 550 or 650 °C in a vacuum environment of 6 Pa, using a holding time of 3 min and a pressure of 200 MPa.	0.1 wt%	93% (550°C) >97% (650°C)

Reference	Blending method	Sintering method	CNT content	Relative density
	furnace at 693 K for 10 min to decompose a majority of the surfactant.			
Suárez et al. (2014) [27]	<b>.Colloidal mixing process:</b> Merging of the dispersion of the CNTs in an ultrasound bath with ethylene glycol and the subsequent addition of Ni powder. The CNT concentration is 0.2 mg/ml. After 10min in the ultrasound bath, the resulting solution was stirred to homogenize the mixture and then dried in a ventilated furnace. The powder is finally milled in an agate mortar.	<b>CPS or HUP:</b> Consolidated with an axial pressure of 990 MPa. Then densified by pressureless sintering (CPS) under vacuum (1 Pa) at 1223 K for 2.5 h. The second set is densified in a hot uniaxial press (HUP) under vacuum (0.1 Pa) at 1023 K also for 2.5 h.	1 wt% 2 wt% 3 wt% 5 wt%	95.5% (CPS) 98% (HUP)
Suárez et al. (2014) [28]	<b>.Colloidal mixing process:</b> Merging of the dispersion of the CNTs in an ultrasound bath with ethylene glycol and the subsequent addition of Ni powder. The CNT concentration is 0.2 mg/ml. After 10 min in the ultrasound bath, the resulting solution was stirred to homogenize the mixture and then dried in a ventilated furnace. The powder is finally milled in an agate mortar.	<b>CPS:</b> Cold pressed at 990 MPa. Then sintered at 950 °C for 2.5 h in vacuum.	1 wt% (6.5 vol%) 2 wt% (12 vol%) 3 wt% (18 vol%) 5 wt% (27 vol%)	XXX
Suárez et al. (2014) [29]	<b>.Colloidal mixing process:</b> Merging of the dispersion of the CNTs in an ultrasound bath with ethylene glycol and the subsequent addition of Ni powder. The CNT concentration is 0.2 mg/ml. After 10min in the ultrasound bath, the resulting solution was stirred to homogenize the mixture and then dried in a ventilated furnace. The powder	<b>HUP:</b> Cold pressed with 990 MPa and then sintered in under vacuum (0.2 Pa) for 2.5 h at 750°C with a 264 MPa axial pressure.	1 wt% (6.5 vol%) 2 wt% (12 vol%) 3 wt% (18 vol%) 5 wt% (27 vol%)	Up to 99%



Reference	Blending method	Sintering method	CNT content	Relative density
	is finally milled in an agate mortar.			
Rossi et al. (2014) [49]	<b>Colloidal mixing process:</b> Merging of the dispersion of the CNTs in an ultrasound bath with ethylene glycol and the subsequent addition of Ni powder. The CNT concentration is 0.2 mg/ml. After 10min in the ultrasound bath, the resulting solution was stirred to homogenize the mixture and then dried in a ventilated furnace. The powder is finally milled in an agate mortar.	<b>HUP:</b> Cold pressed with 990 MPa and then sintered in under vacuum (0.2 Pa) for 2.5 h at 750°C with a 264 MPa axial pressure.	1 wt% (6.5 vol%) 2 wt% (12 vol%) 3 wt% (18 vol%)	XXX
Suárez et al. (2015) [31]	<b>Colloidal mixing process:</b> Dispersion of CNTs in ethylene glycol (0.2 mg/ml) is mixed in an ultrasound bath with the metallic powders for 20 min and then evaporated to obtain a metal–CNT blend.	<b>HUP and HPT:</b> Sintered in vacuum (0.1 Pa) for 2.5 h at 750°C at a compacting pressure of 264 MPa. The densified composites were further processed at room temperature inducing severe plastic deformation by HPT with 4 rotations applying a 4 GPa pressure. For the thermal stability studies, the HPT-processed samples are annealed at 573 K with a heating rate of 20°C/min and a dwell time of 3 h.	1 wt% 3 wt%	XXX
Reinert et al. (2015) [30]	<b>Colloidal mixing process:</b> CNT concentration in ethylene glycol is 0.006 vol%. A homogenizer (5-min treatment) combined with an ultrasonic bath (20-min treatment) is used for the dispersion of the CNTs. After that, Ni powder is added and mixed with the CNT	<b>HUP:</b> Pre-compacted at 990 MPa. Then sintered in a hot uniaxial press (axial pressure of 264 MPa) in vacuum (0.2 Pa) at 750°C for 2.5 h.	6.5 vol%	98%

Reference	Blending method	Sintering method	CNT content Relative density
	dispersion for 5 min using the homogenizer. Finally, the solvent is evaporated at 150°C in a furnace.		

**Table 3.** Summary of blending and sintering methods for the production of Ni/CNT composites.

## 4.2. Distribution and interaction with the matrix material

As observed in the other metal-CNT systems, agglomeration is observed in all cases. If the different blending methods are considered, it is very unlikely to obtain a predominantly individual CNT dispersion rather than a homogeneous cluster distribution. Nevertheless, this cluster distribution provides also diverse improvements with regard to microstructural refinement and properties enhancement. Furthermore, when the initial agglomerate size (as-received state) is considered, all dispersion methods render very good disaggregation. Regarding the damage to the CNTs during processing, it is clear that highly energetic processing as ball milling increases the amount of defects on the CNTs, whereas milder processing routes as colloidal mixing present a fairly unmodified state of the CNTs structure. Interestingly, the sintering process tends to help in the defect healing [29]. The application of temperature in a non-reactive environment (vacuum sintering of non-carbide forming metal matrices) diminishes the  $I_D/I_G$  ratio as observed with Raman spectroscopy. Furthermore, the purity index  $I_G/I_D$  also is reduced, evidencing some sort of contaminant removal (e.g. amorphous carbon).

Nickel does not form stable carbides [101]; however, it has been reported that under certain conditions it is possible to obtain  $Ni_3C$  [102]. This carbide is brittle and, despite improving the interfacial cohesion to the CNTs, would have a detrimental influence on the transport properties of the composite. Due to its metastable nature, it is quite complex to detect it in the composite. It has been shown that the most suitable way is to assess the crystallographic lattice of the Ni in the vicinity of the CNT-containing areas by selected area electron diffraction [29,102]. In the case of a C-Ni reaction, the originally FCC Ni phase would transition to an intermediate  $Ni_3C$  (hcp) and later would stabilize in an hcp Ni phase. Thus, if this hcp lattice is detected in the near region of the CNT zones, it would mean that the  $Ni_3C$  was previously present. To the date,  $Ni_3C$  in Ni-CNT systems has been only detected once by Hwang et al. [102] under a very specific set of synthesis conditions.

Yamanaka et al. and Nguyen et al. show that the application of SPS rendered a very smooth interface between the CNTs and the matrix [46,48]. This was also observed in HR-TEM for hot pressed samples [29]. In general, all the different approaches have resulted in seamless interfaces that are later translated in improved mechanical properties [26,48], thermal properties [46], tribological [27,37] and thermal expansion behaviour [47,78]. Additionally, a proper interface would favour a grain boundary drag that improves the microstructural control by achieving refined microstructures [26,28,48].

## 5. Outlook

Although a large amount of efforts was directed towards the development of CNT-MMCs systems, there is still a significant room for improvement. This statement is supported by the fact that as described, dissimilar results have been obtained by even using the same processing methods as well as the same type and amount of CNTs. This is generated by a scarcity of proper knowledge of each particular system. As an example, there is still an ongoing discussion in the community about the most suitable dispersion and blending methods for a certain application. Furthermore, it can be noticed that the impact of interphases on the physical properties of the composites is still not well understood. Thus, we foresee a very high potential to gain new insights on each particular system and subsequently achieve further developments in this field.

## Acknowledgements

The present work is supported by funding from the Deutsche Forschungsgemeinschaft (DFG, projects: MU 959/38-1 and SU 911/1-1). The authors wish to acknowledge the EFRE Funds of the European Commission for support of activities. This work was also supported by the CREATE-Network Project, Horizon 2020 of the European Commission (RISE Project No. 644013).

## Author details

Sebastian Suárez\*, Leander Reinert and Frank Mücklich

\*Address all correspondence to: s.suarez@mx.uni-saarland.de

Functional Materials, Dept. of Materials Science and Engineering, Saarland University, Germany.

## References

- [1] Ramakrishna S, Mayer J, Wintermantel E, et al. Biomedical applications of polymer-composite materials: A review. *Compos Sci Technol* 2001; 61: 1189–1224.
- [2] Scholz MS, Blanchfield JP, Bloom LD, et al. The use of composite materials in modern orthopaedic medicine and prosthetic devices: A review. *Compos Sci Technol* 2011; 71: 1791–1803.

- [3] Cavalier JC, Berdoyes I, Bouillon E. Composites in Aerospace Industry. *Adv Sci Technol* 2006; 50: 153–162.
- [4] Jorio A, Dresselhaus M, Dresselhaus G. *Carbon Nanotubes: Advanced topics in the synthesis, structure, properties and applications*. Heidelberg, DE: Springer-Verlag, 2008.
- [5] Prasek J, Drbohlavova J, Chomoucka J, et al. Methods for carbon nanotubes synthesis –review. *J Mater Chem* 2011; 21: 15872.
- [6] Guiderdoni C, Pavlenko E, Turq V, et al. The preparation of carbon nanotube (CNT)/copper composites and the effect of the number of CNT walls on their hardness, friction and wear properties. *Carbon* 2013; 58: 185–197.
- [7] Xue ZW, Wang LD, Zhao PT, et al. Microstructures and tensile behavior of carbon nanotubes reinforced Cu matrix composites with molecular-level dispersion. *Mater & Des* 2012; 34: 298–301.
- [8] Xu W, Hu R, Li J, et al. Effect of electrical current on tribological property of Cu matrix composite reinforced by carbon nanotubes. *Trans Nonferrous Met Soc China* 2011; 21: 2237–2241.
- [9] Kim KT, Cha S Il, Gemming T, et al. The role of interfacial oxygen atoms in the enhanced mechanical properties of carbon-nanotube-reinforced metal matrix nanocomposites. *Small* 2008; 4: 1936–1940.
- [10] Shukla AK, Nayan N, Murty SVSN, et al. On the Possibility of Occurrence of Anisotropy in Processing of Cu-CNT Composites by Powder Metallurgical Techniques. *Mater Sci Forum* 2012; 710: 285–290.
- [11] Kim KT, Eckert J, Menzel SB, et al. Grain refinement assisted strengthening of carbon nanotube reinforced copper matrix nanocomposites. *Appl Phys Lett* 2008; 92: 121901.
- [12] Daoush WM. Processing and characterization of CNT/Cu nanocomposites by powder technology. *Powder Metall Met Ceram* 2009; 47: 531–537.
- [13] Dai P-Q, Xu W-C, Huang Q-Y. Mechanical properties and microstructure of nanocrystalline nickel-carbon nanotube composites produced by electrode position. *Mater Sci Eng A* 2008; 483-484: 172–174.
- [14] Firkowska I, Boden A, Vogt A-M, et al. Effect of carbon nanotube surface modification on thermal properties of copper-CNT composites. *J Mater Chem* 2011; 21: 17541–17546.
- [15] Chai G, Sun Y, Sun J ‘Jenny’, et al. Mechanical properties of carbon nanotube–copper nanocomposites. *J Micromechanics Microengineering* 2008; 18: 035013.
- [16] Sule R, Olubambi P A., Sigalas I, et al. Spark plasma sintering of sub-micron copper reinforced with ruthenium–carbon nanotube composites for thermal management applications. *Synth Met* 2015; 202: 123–132.

- [17] Chen B, Yang J, Zhang Q, et al. Tribological properties of copper-based composites with copper coated NbSe<sub>2</sub> and CNT. *Mater Des* 2015; 75: 24–31.
- [18] Kwon H, Estili M, Takagi K, et al. Combination of hot extrusion and spark plasma sintering for producing carbon nanotube reinforced aluminum matrix composites. *Carbon* 2009; 47: 570–577.
- [19] Kwon H, Bradbury CR, Leparoux M. Fabrication of Functionally Graded Carbon Nanotube-Reinforced Aluminum Matrix Composite. *Adv Eng Mater* 2011; 13: 325–329.
- [20] Jiang L, Li Z, Fan G, et al. The use of flake powder metallurgy to produce carbon nanotube (CNT)/aluminum composites with a homogenous CNT distribution. *Carbon* 2012; 50: 1993–1998.
- [21] Kwon H, Takamichi M, Kawasaki A, et al. Investigation of the interfacial phases formed between carbon nanotubes and aluminum in a bulk material. *Mater Chem Phys* 2013; 138: 787–793.
- [22] Phuong DD, Trinh P Van, An N Van, et al. Effects of carbon nanotube content and annealing temperature on the hardness of CNT reinforced aluminum nanocomposites processed by the high pressure torsion technique. *J Alloys Compd* 2014; 613: 68–73.
- [23] Chen B, Kondoh K, Imai H, et al. Simultaneously enhancing strength and ductility of carbon nanotube/aluminum composites by improving bonding conditions. *Scr Mater* 2016; 113: 158–162.
- [24] Borkar T, Hwang J, Hwang JY, et al. Strength versus ductility in carbon nanotube reinforced nickel matrix nanocomposites. *J Mater Res* 2014; 29: 761–769.
- [25] Hwang JY, Lim BK, Tiley J, et al. Interface analysis of ultra-high strength carbon nanotube/nickel composites processed by molecular level mixing. *Carbon* 2013; 57: 282–287.
- [26] Suarez S, Lasserre F, Mücklich F. Mechanical properties of MWNT/Ni bulk composites: Influence of the microstructural refinement on the hardness. *Mater Sci Eng A* 2013; 587: 381–386.
- [27] Suárez S, Rosenkranz A, Gachot C, et al. Enhanced tribological properties of MWCNT/Ni bulk composites – Influence of processing on friction and wear behaviour. *Carbon* 2014; 66: 164–171.
- [28] Suárez S, Ramos-Moore E, Lechthaler B, et al. Grain growth analysis of multiwalled carbon nanotube-reinforced bulk Ni composites. *Carbon* 2014; 70: 173–178.
- [29] Suarez S, Lasserre F, Prat O, et al. Processing and interfacial reaction evaluation in MWCNT/Ni composites. *Phys Status Solidi* 2014; 211: 1555–1561.
- [30] Reinert L, Zeiger M, Suarez S, et al. Dispersion analysis of carbon nanotubes, carbon onions, and nanodiamonds for their application as reinforcement phase in nickel metal matrix composites. *RSC Adv* 2015; 5: 95149–95159.

- [31] Suarez S, Lasserre F, Soldera F, et al. Microstructural thermal stability of CNT-reinforced composites processed by severe plastic deformation. *Mater Sci Eng A* 2015; 626: 122–127.
- [32] Jenei P, Gubicza J, Yoon EY, et al. High temperature thermal stability of pure copper and copper-carbon nanotube composites consolidated by High Pressure Torsion. *Compos Part A Appl Sci Manuf* 2013; 51: 71–79.
- [33] Jenei P, Yoon EY, Gubicza J, et al. Microstructure and hardness of copper–carbon nanotube composites consolidated by High Pressure Torsion. *Mater Sci Eng A* 2011; 528: 4690–4695.
- [34] Pham VT, Bui HT, Tran BT, et al. The effect of sintering temperature on the mechanical properties of a Cu/CNT nanocomposite prepared via a powder metallurgy method. *Adv Nat Sci Nanosci Nanotechnol* 2011; 2: 015006.
- [35] Chen WX, Tu JP, Wang LY, et al. Tribological application of carbon nanotubes in a metal-based composite coating and composites. *Carbon* 2003; 41: 215–222.
- [36] Hwang J, Singh A, Banerjee R, et al. Processing and thermal conductivity of carbon nanotube-reinforced nickel matrix composites. *ASME Summer Heat Transf Conf* 2009; 1–4.
- [37] Scharf TW, Neira A, Hwang JY, et al. Self-lubricating carbon nanotube reinforced nickel matrix composites. *J Appl Phys* 2009; 106: 013508.
- [38] Singh A. RP, Hwang JY, Scharf TW, et al. Bulk nickel–carbon nanotube nanocomposites by laser deposition. *Mater Sci Technol* 2010; 26: 1393–1400.
- [39] Xu C, Wei B, Ma R, et al. Fabrication of aluminum-carbon nanotube composites and their electrical properties. *Carbon* 1999; 37: 855–858.
- [40] Kuzumaki T, Miyazawa K, Ichinose H, et al. Processing of carbon nanotube reinforced aluminium composite. *J Mater Res* 1998; 13: 2445–2449.
- [41] Tokunaga T, Kaneko K, Horita Z. Production of aluminum-matrix carbon nanotube composite using high pressure torsion. *Mater Sci Eng A* 2008; 490: 300–304.
- [42] Cho S, Kikuchi K, Miyazaki T, et al. Multiwalled carbon nanotubes as a contributing reinforcement phase for the improvement of thermal conductivity in copper matrix composites. *Scr Mater* 2010; 63: 375–378.
- [43] Rajkumar K, Aravindan S. Tribological studies on microwave sintered copper–carbon nanotube composites. *Wear* 2011; 270: 613–621.
- [44] Guiderdoni C, Estournès C, Peigney a., et al. The preparation of double-walled carbon nanotube/Cu composites by spark plasma sintering, and their hardness and friction properties. *Carbon* 2011; 49: 4535–4543.



- [45] Sule R, Olubambi PA, Sigalas I, et al. Effect of SPS consolidation parameters on submicron Cu and Cu–CNT composites for thermal management. *Powder Technol* 2014; 258: 198–205.
- [46] Yamanaka S, Gonda R, Kawasaki A, et al. Fabrication and thermal properties of carbon nanotube/nickel composite by spark plasma sintering method. *Mater Trans* 2007; 48: 2506–2512.
- [47] Suárez S, Soldera F, Oliver CG, et al. Thermomechanical Behavior of Bulk Ni/MWNT Composites Produced via Powder Metallurgy. *Adv Eng Mater* 2012; 14: 499–502.
- [48] Nguyen J, Holland TB, Wen H, et al. Mechanical behavior of ultrafine-grained Ni-carbon nanotube composite. *J Mater Sci* 2014; 49: 2070–2077.
- [49] Rossi P, Suarez S, Soldera F, et al. Quantitative Assessment of the Reinforcement Distribution Homogeneity in CNT/Metal Composites. *Adv Eng Mater* 2015; 17: 1017–1021.
- [50] Nam DH, Kim YK, Cha SI, et al. Effect of CNTs on precipitation hardening behavior of CNT/Al–Cu composites. *Carbon* 2012; 50: 4809–4814.
- [51] Kim KT, Cha S II, Hong SH. Hardness and wear resistance of carbon nanotube reinforced Cu matrix nanocomposites. *Mater Sci Eng A* 2007; 449–451: 46–50.
- [52] Kim KT, Eckert J, Liu G, et al. Influence of embedded-carbon nanotubes on the thermal properties of copper matrix nanocomposites processed by molecular-level mixing. *Scr Mater* 2011; 64: 181–184.
- [53] Lal M, Singhal SK, Sharma I, et al. An alternative improved method for the homogeneous dispersion of CNTs in Cu matrix for the fabrication of Cu/CNTs composites. *Appl Nanosci* 2012; 3: 29–35.
- [54] Tsai P-C, Jeng Y-R. Experimental and numerical investigation into the effect of carbon nanotube buckling on the reinforcement of CNT/Cu composites. *Compos Sci Technol* 2013; 79: 28–34.
- [55] Chu K, Guo H, Jia C, et al. Thermal properties of carbon nanotube-copper composites for thermal management applications. *Nanoscale Res Lett* 2010; 5: 868–874.
- [56] Liu Q, Ke L, Liu F, et al. Microstructure and mechanical property of multi-walled carbon nanotubes reinforced aluminum matrix composites fabricated by friction stir processing. *Mater Des* 2013; 45: 343–348.
- [57] Isaza Merino C A., Meza Meza JM, Sierra Gallego G a. A Novel Technique for Production of Metal Matrix Composites Reinforced With Carbon Nanotubes. *J Manuf Sci Eng* 2016; 138: 024501–1/5.
- [58] Esawi AMK, Morsi K, Sayed A, et al. Fabrication and properties of dispersed carbon nanotube–aluminum composites. *Mater Sci Eng A* 2009; 508: 167–173.

- [59] Choi HJ, Min BH, Shin JH, et al. Strengthening in nanostructured 2024 aluminum alloy and its composites containing carbon nanotubes. *Compos Part A Appl Sci Manuf* 2011; 42: 1438–1444.
- [60] Choi HJ, Shin JH, Bae DH. Grain size effect on the strengthening behavior of aluminum-based composites containing multi-walled carbon nanotubes. *Compos Sci Technol* 2011; 71: 1699–1705.
- [61] Asgharzadeh H, Joo S-H, Kim HS. Consolidation of Carbon Nanotube Reinforced Aluminum Matrix Composites by High-Pressure Torsion. *Metall Mater Trans A* 2014; 45: 4129–4137.
- [62] Carvalho O, Miranda G, Soares D, et al. Carbon nanotube dispersion in aluminum matrix composites — Quantification and influence on strength. *Mech Adv Mater Struct* 2016; 23: 66–73.
- [63] Tu JP, Yang YZ, Wang LY, et al. Tribological properties of carbon-nanotube-reinforced copper composites. *Tribol Lett* 2001; 10: 225–228.
- [64] Kim KT, Cha S Il, Hong SH. Microstructures and tensile behavior of carbon nanotube reinforced Cu matrix nanocomposites. *Mater Sci Eng A* 2007; 448-451: 46–50.
- [65] Li H, Misra A, Zhu Y, et al. Processing and characterization of nanostructured Cu-carbon nanotube composites. *Mater Sci Eng A* 2009; 523: 60–64.
- [66] Li H, Misra A, Horita Z, et al. Strong and ductile nanostructured Cu-carbon nanotube composite. *Appl Phys Lett* 2009; 95: 25–27.
- [67] Uddin SM, Mahmud T, Wolf C, et al. Effect of size and shape of metal particles to improve hardness and electrical properties of carbon nanotube reinforced copper and copper alloy composites. *Compos Sci Technol* 2010; 70: 2253–2257.
- [68] Chu K, Jia C, Li W, et al. Mechanical and electrical properties of carbon-nanotube-reinforced Cu-Ti alloy matrix composites. *Phys Status Solidi* 2013; 210: 594–599.
- [69] Shukla a. K, Nayan N, Murty SVSN, et al. Processing of copper-carbon nanotube composites by vacuum hot pressing technique. *Mater Sci Eng A* 2013; 560: 365–371.
- [70] Chu K, Jia C, Jiang L, et al. Improvement of interface and mechanical properties in carbon nanotube reinforced Cu–Cr matrix composites. *Mater Des* 2013; 45: 407–411.
- [71] Yoon EY, Lee DJ, Park B, et al. Grain refinement and tensile strength of carbon nanotube-reinforced Cu matrix nanocomposites processed by high-pressure torsion. *Met Mater Int* 2013; 19: 927–932.
- [72] Barzegar Vishlaghi M, Ataie A. Investigation on solid solubility and physical properties of Cu–Fe/CNT nano-composite prepared via mechanical alloying route. *Powder Technol* 2014; 268: 102–109.

- [73] Akbarpour MR, Farvizi M, Lee DJ, et al. Effect of high-pressure torsion on the microstructure and strengthening mechanisms of hot-consolidated Cu–CNT nanocomposite. *Mater Sci Eng A* 2015; 638: 289–295.
- [74] Varo T, Canakci A. Effect of the CNT Content on Microstructure, Physical and Mechanical Properties of Cu-Based Electrical Contact Materials Produced by Flake Powder Metallurgy. *Arab J Sci Eng* 2015; 40: 2711–2720.
- [75] Imai H, Kondoh K, Li S, et al. Microstructural and Electrical Properties of Copper - Titanium Alloy Dispersed with Carbon Nanotubes via Powder Metallurgy Process. *Mater Trans* 2014; 55: 522–527.
- [76] Hwang JY, Neira A, Scharf TW, et al. Laser-deposited carbon nanotube reinforced nickel matrix composites. *Scr Mater* 2008; 59: 487–490.
- [77] Choi H, Shin J, Bae D. The effect of milling conditions on microstructures and mechanical properties of Al/MWCNT composites. *Compos Part A Appl Sci Manuf* 2012; 43: 1061–1072.
- [78] Suárez S, Ramos-Moore E, Mücklich F. A high temperature X-ray diffraction study of the influence of MWCNTs on the thermal expansion of MWCNT/Ni composites. *Carbon* 2013; 51: 404–409.
- [79] Kwon H, Park DH, Silvain JF, et al. Investigation of carbon nanotube reinforced aluminum matrix composite materials. *Compos Sci Technol* 2010; 70: 546–550.
- [80] Sairam K, Sonber JK, Murthy TSRC, et al. Influence of spark plasma sintering parameters on densification and mechanical properties of boron carbide. *Int J Refract Met Hard Mater* 2014; 42: 185–192.
- [81] Suk-Joong L.Kang. Sintering Densification, Grain Growth, and Microstructure. *Elsevier Butterworth-Heinemann Linacre House* 2005; pp. 9–18.
- [82] Cumings J, Zettl A. Electrical and Mechanical Properties of Nanotubes Determined Using In-situ TEM Probes. In: Rotkin S, Subramoney S (eds) *Applied Physics of Carbon Nanotubes*. Springer, 2005, p. 349.
- [83] Huang Q, Gao L, Liu Y. Sintering and thermal properties of multiwalled carbon nanotube – BaTiO<sub>3</sub> composites. *J Mater Chem* 2005; 1995–2001.
- [84] Lahiri D, Singh V, Keshri AK, et al. Carbon nanotube toughened hydroxyapatite by spark plasma sintering: Microstructural evolution and multiscale tribological properties. *Carbon* 2010; 48: 3103–3120.
- [85] Zhan G-D, Kuntz JD, Wan J, et al. Single-wall carbon nanotubes as attractive toughening agents in alumina-based nanocomposites. *Nat Mater* 2003; 2: 38–42.
- [86] Hu N, Jia B, Arai M, et al. Prediction of thermal expansion properties of carbon nanotubes using molecular dynamics simulations. *Comput Mater Sci* 2012; 54: 249–254.

- [87] Kwon Y-K, Berber S, Tománek D. Thermal Contraction of Carbon Fullerenes and Nanotubes. *Phys Rev Lett* 2004; 92: 015901.
- [88] Berber S, Kwon Y, Tomanek D. Unusually high thermal conductivity of carbon nanotubes. *Phys Rev Lett* 2000; 84: 4613–6.
- [89] Kim P, Shi L, Majumdar A., et al. Thermal Transport Measurements of Individual Multiwalled Nanotubes. *Phys Rev Lett* 2001; 87: 19–22.
- [90] Poncharal P, Berger C, Yi Y, et al. Room temperature ballistic conduction in carbon nanotubes. *J Phys Chem B* 2002; 106: 12104–12118.
- [91] Poncharal P, Frank S, Wang ZL, et al. Conductance quantization in multiwalled carbon nanotubes. *Eur Phys J D* 1999; 9: 77–79.
- [92] Hone J, Llaguno MC, Nemes NM, et al. Electrical and thermal transport properties of magnetically aligned single wall carbon nanotube films. *Appl Phys Lett* 2000; 77: 666–668.
- [93] Bakshi SR, Batista RG, Agarwal A. Quantification of carbon nanotube distribution and property correlation in nanocomposites. *Compos Part A Appl Sci Manuf* 2009; 40: 1311–1318.
- [94] Bakshi SR, Lahiri D, Agarwal A. Carbon nanotube reinforced metal matrix composites - a review. *Int Mater Rev* 2010; 55: 41–64.
- [95] Agarwal A, Bakshi SR, Lahiri D. *Carbon Nanotubes reinforced Metal Matrix Composites*. 1st ed. Boca Raton, FL, USA: CRC Press, 2011.
- [96] Okamoto H. Phase Diagram Updates: Section III: Al-C (Aluminum-Carbon). *J Phase Equilibria* 1992; 13: 97–98.
- [97] Lee J, Novikov N (eds). *Innovative superhard materials and sustainable coatings for advanced manufacturing*. Dordrecht, The Netherlands: Springer - NATO Science Series, 2005.
- [98] Foster LM, Long G, Hunter MS. Reactions Between Aluminum Oxide and Carbon The  $\text{Al}_2\text{O}_3$ — $\text{Al}_4\text{C}_3$  Phase Diagram. *J Am Ceram Soc* 1956; 39: 1–11.
- [99] Yamada Y, Castleman Jr AW. Gas-phase copper carbide clusters. *Chem Phys Lett* 1993; 204: 133–138.
- [100] Park M, Kim BH, Kim S, et al. Improved binding between copper and carbon nanotubes in a composite using oxygen-containing functional groups. *Carbon* 2011; 49: 811–818.
- [101] Singleton M, Nash P. The C-Ni (Carbon-Nickel) system. *Bull Alloy Phase Diagrams* 1989; 10: 121–126.
- [102] Hwang JY, Singh ARP, Chaudhari M, et al. Templated Growth of Hexagonal Nickel Carbide Nanocrystals on Vertically Aligned Carbon Nanotubes. *J Phys Chem C* 2010; 114: 10424–10429.

